JAERI-Tech
97-032

EXPERIMENTAL STUDY ON HEAT TRANSFER AUGMENTATION FOR HIGH HEAT FLUX REMOVAL IN RIB-ROUGHENED NARROW CHANNELS

July 1997

Md. Shafiqul ISLAM*, Ryutaro HINO, Katsuhiro HAGA
Masanori MONDE* and Yukio SUDO

日本原子力研究所
Japan Atomic Energy Research Institute

本レポートは，日本原子力研究所が不定期に公刊している研究報告書です。
入手の問合わせは，日本原子力研究所研究情報部研究情報課（〒319-11　茨城県那珂郡東海村）あて，お申し越しください。なお，このほかに財団法人原子力公済会資料センター（〒319-11　茨城県那珂郡東海村日本原子力研究所内）で複写による実費頒布をおこなっております。

This report is issued irregularly.
Inquiries about availability of the reports should be addressed to Research Information Division, Department of Intellectual Resources, Japan Atomic Energy Research Institute, Tokai-mura, Naka-gun, Ibaraki-ken 319-11, Japan.

編集兼発行　日本原子力研究所
印　　刷　㈱高野高速印刷

Experimental Study on Heat Transfer Augmentation for High Heat Flux Removal in Rib-roughened Narrow Channels

Md. Shafiqul ISLAM*, Ryutaro HINO, Katsuhiro HAGA+
Masanori MONDE* and Yukio SUDO++

Center for Neutron Science
Tokai Research Establishment
Japan Atomic Energy Research Institute
Tokai-mura, Naka-gun, Ibaraki-ken

(Received June 11, 1997)

Frictional pressure drop and heat transfer performance in a very narrow rectangular channel having one-sided constant heat flux and repeated-ribs for turbulent flow have been investigated experimentally, and their experimental correlations were obtained using the least square method. The rib pitch-to-height ratios(p/k) were 10 and 20 while holding the rib hgight constant at 0.2mm, the Reynolds number(Re) from 2,414 to 98,458 under different channel heights of 1.2mm, 2.97mm, and 3.24mm, the rib height-to-channel equivalent diameter(k/De) of 0.03, 0.04, and 0.09 respectively. The results show that the rib-roughened surface augments heat transfer 2-3 times higher than that of the smooth surface with the expense of 2.8-4 times higher frictional pressure drop under Re=5000-10^5, p/k=10, and H=1.2mm. Experimental results obtained by channel height, H=1.2mm shows a little bit higher heat transfer and friction factor performance than the higher channel height, H=3.24mm. The effect of fin and consequently higher turbulence intensity are responsible for producing higher heat transfer rates. The obtained correlations could be used to design the cooling passages between the target plates to remove high heat flux up to 12MW/m^2 generated at target plates in a high-intensity proton accelerator system.

Keywords : Narrow Channel, Heat Transfer Augmentation, Rib-Roughened Surface, Correlations, Turbulence Intensity, Cooling Passage, High Heat Flux, Target Plate

+ Department of Advanced Nuclear Heat Technology, Oarai Research Establishment
++ Office of Planning
* Saga University

リブ付き狭隘流路における熱伝達促進に関する実験的研究

日本原子力研究所東海研究所中性子科学研究センター
Md. Shafiqul Islam* ・日野竜太郎・羽賀　勝洋+
門出　政則*・数土　幸夫++

（１９９７年６月１１日受理）

片面均一加熱の矩形リブ付き狭隘流路の乱流域における摩擦損失計数と熱伝達率を実験的に調べ，実験データを基にしてそれらの実験式を導出した。実験は，リブピッチと高さの比(P/K)が10及び20（リブ高さは0.2mm）の条件で，流路高さ(H)を1.2mm，2.97mm，3.24mmと変えて行った。このときのレイノルズ(Re)数範囲は2414～98458，リブ高さと等価直径の比(k/De)は0.03，0.04，0.09であった。熱伝達率はリブのない平滑な流路よりも２倍以上向上するが，Re数が5000以上で，p/kが10，流路高さが1.2mmの場合には，圧力損失が2.8～4倍増大した。流路高さが1.2mmの実験結果は，H=3.24mmの場合よりも高い熱伝達率と摩擦損失係数を示した。これはリブの効果，すなわち，より高い乱流強度の発生が熱伝達率の向上を促しているものと考えられる。導出した熱伝達率及び摩擦損失係数の実験式は，大強度陽子加速器システムにおいてターゲット板に発生する12MW/m^{2}の高熱流束を除去するためのターゲット冷却材流路の設計に役立つものと考えられる。

東海研究所：〒319-11　茨城県那珂郡東海村白方白根2-4
+　大洗研究所核熱利用研究部
++ 企画室
*　佐賀大学

Contents

目　　次

1. Introduction

Surfaces roughened from one side with discrete small square ribs in very narrow channels whose heights are so small as approximately 1 to 3 mm that are similar to the gaps between the target plates could be introduced to remove high heat flux up to 12 MW/m^2 generated at target plates in a high-intensity proton accelerator system. The high-intensity proton accelerator of 1.5 GeV and 1mA with a beam power of 1.5 MW is connected with a target and is now under designing at Japan Atomic Energy Research Institute (JAERI) for contributing to neutron science. The target consists of heavy metal plates such as, tungsten and these are cooled by water. In designing, heat transfer augmentation is very much important to keep the surface temperature of target plates below 200℃ from the view point of safety and extending its life.

Surface roughness with repeated-rib promoters is a well established method. The ribs break the viscous sublayer and create local wall turbulence due to flow separation and reattachment between the ribs, which greatly augment heat transfer,usually with an increase in the flow friction and pressure drop. Developing and fully developed turbulence heat transfer and friction in narrow rectangular channels with rib turbulators on one-sided have been studied experimentally. The effects of rib height, rib spacing and rib shape on heat transfer coefficients and friction factors over a wide range of Reynolds numbers have been well established for the very narrow rectangular channels. Empirical friction and heat transfer correlations have been developed for heat transfer designers. However, heat transfer designers are continually seeking the high-performance enhanced surface. The concept of turbulence promoters was examined for this current study. It is of interest how the surface with rougheners can perform better than the surface without rougheners(smooth). The objective of this study is to investigate the following topics on heat removal phenomena of the solid targets.

1) the effect of flow conditions such as, inlet water temperature and velocity
2) the effect of gap size from 1 mm to 3 mm,
3) heat transfer and pressure loss coefficients for single-phase flow under constant heat rate condition.

Such a very narrow channel with one-sided repeated-rib promoters with one-sided constant heat flux condition can play a predominent role in achieving this

goal. Twelve narrow rectangular channels were tested where four of them were smooth and the remaining eight were rib-roughened from one side. Half of the total test sections were tested under heating and remaining without heating conditions at varying channels heights. The rib pitch-to-height ratios (p/k) were 10 and 20 while holding the rib height constant at 0.2 mm, the Reynolds number (Re) from 2,414 to 98,485 under different channel heights of 1.2 mm, 2.97 mm, and 3.24 mm, the rib height-to-channel equivalent diameter (k/D_e) of 0.03, 0.04, and 0.09 respectively. The various investigations carried out on internally augmented tubes including major information are listed in chap. 2.

2. Literature Survey

Improvements of heat transfer performance through passive and active augmentation methods have been studied intensively for over three decades. Heat exchangers with single-phase tube-side flow are one of the important applications where passive surface-modification methods are popularly employed. Typical examples of passive augmentation are surface roughness, displaced promoters and vortex generators. Ribs, indentations, spiral flutes, and coil inserts are some common surface modification techniques that are effective for many applications, and can be used conveniently for retubing existing heat exchangers. With the passage of time, the above types of surface roughness are being utilized more and more for augmentation of heat transfer. These methods are used to improve heat transfer coefficients inside tubes or out side tubes or rods. Active augmentation, which has also been studied extensively, requires the addition of external power to bring about the desired flow modification. Examples include heat transfer surface vibration, fluid vibration, and electrostatic field introduction, are costly and complex. Of these, the most well-known method for augmentation heat transfer is to roughen the surface using repeated-ribs, since these are relatively easy to manufacture, and its simplicity in application. Many investigations have been carried out both analytically and experimentally on tubes and annuli under air-flow conditions where very few studies are on narrow rectangular channels. There are almost no heat transfer data both analytically and experimentally on a very narrow rectangular channel with one-sided repeated-ribs and one-sided constant heat flux under water-flow conditions.

goal. Twelve narrow rectangular channels were tested where four of them were smooth and the remaining eight were rib-roughened from one side. Half of the total test sections were tested under heating and remaining without heating conditions at varying channels heights. The rib pitch-to-height ratios (p/k) were 10 and 20 while holding the rib height constant at 0.2 mm, the Reynolds number (Re) from 2,414 to 98,485 under different channel heights of 1.2 mm, 2.97 mm, and 3.24 mm, the rib height-to-channel equivalent diameter (k/D_e) of 0.03, 0.04, and 0.09 respectively. The various investigations carried out on internally augmented tubes including major information are listed in chap. 2.

2. Literature Survey

Improvements of heat transfer performance through passive and active augmentation methods have been studied intensively for over three decades. Heat exchangers with single-phase tube-side flow are one of the important applications where passive surface-modification methods are popularly employed. Typical examples of passive augmentation are surface roughness, displaced promoters and vortex generators. Ribs, indentations, spiral flutes, and coil inserts are some common surface modification techniques that are effective for many applications, and can be used conveniently for retubing existing heat exchangers. With the passage of time, the above types of surface roughness are being utilized more and more for augmentation of heat transfer. These methods are used to improve heat transfer coefficients inside tubes or out side tubes or rods. Active augmentation, which has also been studied extensively, requires the addition of external power to bring about the desired flow modification. Examples include heat transfer surface vibration, fluid vibration, and electrostatic field introduction, are costly and complex. Of these, the most well-known method for augmentation heat transfer is to roughen the surface using repeated-ribs, since these are relatively easy to manufacture, and its simplicity in application. Many investigations have been carried out both analytically and experimentally on tubes and annuli under air-flow conditions where very few studies are on narrow rectangular channels. There are almost no heat transfer data both analytically and experimentally on a very narrow rectangular channel with one-sided repeated-ribs and one-sided constant heat flux under water-flow conditions.

A comprehensive list was prepared consisting of all the experimental investigations from which heat transfer and friction factor data could be extracted for different roughened surfaces for single-phase turbulent flow in internally augmented tubes up to now. No restrictions were placed on the flow parameters, namely, the Reynolds number and the Prandtl number, even though much of the data were obtained in the turbulent regime with either air or water as the test fluid. This file lists the authors of the investigation and the type of enhanced tubes along with number of tubes tested in the experiments, which are summarized in Table1. The sources are listed in the reference section. In addition, the type of experiment, whether the fluid is heated or cooled, and the method of heat transfer are provided whenever possible for future reference. The objective of this list is to make clear that our experiment will be the first step to augment high heat transfer performance in a very narrow rectangular channel with one-sided repeated square ribs, and one-sided constant heat flux under water-flow conditions.

3. Heat Transfer Augmentation

Different techniques are available to augment the heat transfer performance. The most well-known augmentative techniques are as follows :

a. Surface promoters
b. Displaced promoters
c. Vortex flow

Surface roughness is one of the promising techniques to be considered seriously as a means of augmenting forced-convection with single-phase flow heat transfer. Initially it was speculated that elevated heat transfer coefficients might accompany the relatively high friction factors characteristic of rough conduits. However, since the commercial roughness is not well defined, artificial surface roughness - introduced through knurling or threading or formed by repeated-rib promoters has been employed. Although the augmented heat transfer with surface promoters is often due in part to the fin effect, it is difficult to separate the fin contribution. For the experimental data discussed in chap. 4, the augmented heat transfer coefficient is referenced to the envelope diameter.

In certain cases it may be desirable to leave the heat transfer surface intact and

A comprehensive list was prepared consisting of all the experimental investigations from which heat transfer and friction factor data could be extracted for different roughened surfaces for single-phase turbulent flow in internally augmented tubes up to now. No restrictions were placed on the flow parameters, namely, the Reynolds number and the Prandtl number, even though much of the data were obtained in the turbulent regime with either air or water as the test fluid. This file lists the authors of the investigation and the type of enhanced tubes along with number of tubes tested in the experiments, which are summarized in Table1. The sources are listed in the reference section. In addition, the type of experiment, whether the fluid is heated or cooled, and the method of heat transfer are provided whenever possible for future reference. The objective of this list is to make clear that our experiment will be the first step to augment high heat transfer performance in a very narrow rectangular channel with one-sided repeated square ribs, and one-sided constant heat flux under water-flow conditions.

3. Heat Transfer Augmentation

Different techniques are available to augment the heat transfer performance. The most well-known augmentative techniques are as follows :

a. Surface promoters
b. Displaced promoters
c. Vortex flow

Surface roughness is one of the promising techniques to be considered seriously as a means of augmenting forced-convection with single-phase flow heat transfer. Initially it was speculated that elevated heat transfer coefficients might accompany the relatively high friction factors characteristic of rough conduits. However, since the commercial roughness is not well defined, artificial surface roughness - introduced through knurling or threading or formed by repeated-rib promoters has been employed. Although the augmented heat transfer with surface promoters is often due in part to the fin effect, it is difficult to separate the fin contribution. For the experimental data discussed in chap. 4, the augmented heat transfer coefficient is referenced to the envelope diameter.

In certain cases it may be desirable to leave the heat transfer surface intact and

achieve the augmentation by disturbing the flow near the heated surface. Displaced promoters alter flow mechanics near the surface by disturbing the core flow and can be done to place thin rings or discs in a tube. It is seen that rings substantially improve heat transfer in the lower Reynolds number range where discs are not particularly effective. Examples are baffles and mixing elements. It has been established that swirling the flow will improve heat transfer in duct flow. Generation of swirl flow has been accomplished by coiled wires, spiral fins, stationary propellers, coiled tubes, inlet vortex generators, and twisted tapes. Virtually all of these arrangements have been shown to improve single-phase and boiling heat transfer at the expense of increased pumping power. Heat transfer coefficients are relatively high for vortex flow due to increased velocity, secondary flow produced by the radial body force when favorable density gradients are present, and a fin effect with certain continuous swirl generators.

Of the several methods discussed above, surface promoters with repeated-ribs are the most popular as they are effective in enhancing the heat transfer, relatively easy to manufacture, and are cost effective for many applications, and was employed at the test section. The ribs break the viscous sublayer thickness and create local wall turbulence due to flow separation and reattachment between the ribs, which greatly augment the heat transfer. It is concluded that the roughness height should exceed the sublayer thickness before it becomes effective. This type of surface roughness is very much effective for augmenting the heat transfer coefficients with the expense of increased frictional pressure drop. The following chapter is concerned with the experiments for the prediction of turbulent friction factors and heat transfer performance in very narrow rectangular channels with repeated-ribs under one-sided constant heat flux condition.

4. Experimental Program

4.1 Test apparatus

The layout of the experimental apparatus and measuring equipment is shown in Fig. 1. It is seen that the closed-loop system incorporates the test section, flow meters, a storage tank, a circulating pump, and a D.C power supplier. Water from the pump was supplied to the test section through the flow meter, and then,

achieve the augmentation by disturbing the flow near the heated surface. Displaced promoters alter flow mechanics near the surface by disturbing the core flow and can be done to place thin rings or discs in a tube. It is seen that rings substantially improve heat transfer in the lower Reynolds number range where discs are not particularly effective. Examples are baffles and mixing elements. It has been established that swirling the flow will improve heat transfer in duct flow. Generation of swirl flow has been accomplished by coiled wires, spiral fins, stationary propellers, coiled tubes, inlet vortex generators, and twisted tapes. Virtually all of these arrangements have been shown to improve single-phase and boiling heat transfer at the expense of increased pumping power. Heat transfer coefficients are relatively high for vortex flow due to increased velocity, secondary flow produced by the radial body force when favorable density gradients are present, and a fin effect with certain continuous swirl generators.

Of the several methods discussed above, surface promoters with repeated-ribs are the most popular as they are effective in enhancing the heat transfer, relatively easy to manufacture, and are cost effective for many applications, and was employed at the test section. The ribs break the viscous sublayer thickness and create local wall turbulence due to flow separation and reattachment between the ribs, which greatly augment the heat transfer. It is concluded that the roughness height should exceed the sublayer thickness before it becomes effective. This type of surface roughness is very much effective for augmenting the heat transfer coefficients with the expense of increased frictional pressure drop. The following chapter is concerned with the experiments for the prediction of turbulent friction factors and heat transfer performance in very narrow rectangular channels with repeated-ribs under one-sided constant heat flux condition.

4. Experimental Program

4.1 Test apparatus

The layout of the experimental apparatus and measuring equipment is shown in Fig. 1. It is seen that the closed-loop system incorporates the test section, flow meters, a storage tank, a circulating pump, and a D.C power supplier. Water from the pump was supplied to the test section through the flow meter, and then,

it passed through a filter, a cooler, the storage tank and a preheater to the pump. The filter was used to filter out solid particles more than 5 μm that may have found their way into the system. A preheater was employed to control the temperature of the working fluid in the test section. The storage tank served as a container into which the working fluid from the test section was discharged, conditioned, and recirculated. The flow rate was measured using two flow meters in parallel and the flow rate through the test section was controlled by adjusting as required a number of valves installed in the circuit. The test section shown in Fig. 2 was 250 mm in length with a varying cross section. Heated length was 200 mm; an entry and exit sections of 25 mm long, were provided a smooth flow out of the test section. The test section consists of a heating surface made of copper plate with an electric heater, glass windows etc. A nichrome plate (0.905 Ω/m) was used as a heater and received electricity from the D.C power supply. Heating of the copper test section was effected by the passage of a high current(0-300A) at voltage(0-60V) through the test specimen. The total heat input to the heating surface was calculated from a knowledge of the current which was measured by a precision ammeter together with the voltage across the heating surface, which was measured with a voltmeter. The ribs were square-type where cross sectional dimension was 0.2 mm×0.2 mm and pitches were 2 or 4 mm.

Figure 3 shows the cross section of flow channel and schematic of flow channel with rib-roughened surface. The cross sectional dimensions can be varied according to channel heights. The width of the test section was 20 mm and channel heights can be varied from 1.2 mm to 3.24 mm. The channel heights found variation from the inlet to the outlet sections and assumed linear variation. The heights were measured by a digital microscope and rechecked by a ultrosonic method. The measuring heights are listed in Figs. (4-6). The major parameters along with *N.H /E.H. conditions of the test section are presented in Table 2. Surface temperature was measured using 26 copper-constantan thermocouples distributed across the span of the copper plates, 2 mm far from the tip of the heating surface, and was recorded by the acquisition system consisting of a data logger and a personal computer. The difference between the two consecutive thermocouples was 8 mm. Three thermocouples of each inlet and outlet of the test section were provided to measure the inlet and outlet

---

*N. H =Non heating E. H = electrical heating

bulk temperatures of water. Eleven differential pressure taps were installed at opposite side of the heating surface to measure the static pressure drop across the test section. The difference between the two consecutive pressure taps was 20 mm. The range and accuracy of the measuring instruments are given in Table 3 and Table 4, respectively. The data, which were obtained under the following experimental conditions are listed in Table 5 .

4.2 Data analysis

The friction factor in a rib-roughened narrow rectangular channel can be determined by measuring the pressure drop across the test section and the flow rate of the water. The friction factor can then be calculated from :

$$f=\triangle P/(2 \times \rho u_m^2/g).(D_e/\triangle L) \quad (1)$$

The friction factor,f is based on isothermal condition (test section without heating). The present friction factor was compared with the friction factor for fully developed turbulent flow in smooth rectangular channels by means of the Blasius correlation :

$$f/f_o = f / [0.079\ Re^{-0.25}] \quad (2)$$

An average outlet temperature of the water was used in the following equation (3) to obtain the net heat transfer rate. The average outlet temperature of the water was obtained by averaging three thermocouples located cross section of the test section at the outlet. The net heat transfer rate can be calculated from :

$$Q= C_p \rho v A_x (T_{out} - T_{in}) \quad (3)$$

The local heat transfer coefficient was calculated from the net heat transfer rate per unit surface area to the heating water, the corrected surface temperature (T_{wc}) on each measured section, and local bulk mean water temperature as :

$$h = Q / A_s(T_{wc} - T_b) \quad (4)$$

where the local temperature (T_w) was read from each cross-sectional thermocouple output. The corrected local surface temperature (T_{wc}) for equation (4) was calculated by one dimensional steady state heat conduction equation as :

$$T_{wc} = T_w - (Q \times \delta) / (A_s \lambda) \quad (5)$$

where the axial and span wise heat conductions were not considered in this

study. The surface area, A_s was based on the smooth surface area, not including an increase of the area due to ribs. Equation (4) was used for the rib-roughened surface and the smooth surface heat transfer coefficient calculations. The maximum heat loss was taken place at the entry and exit of the test section. The local inner wall temperature (T_w) was at maximum 23℃ in the fully developed region at low Reynolds number and smaller channel heights of the test channel. The local inlet bulk water temperature was at best 15℃ depending on the test conditions. The local bulk water temperature, T_b was calculated assuming a linear water temperature rise along the flow channel and is defined as :

$$T_b = T_{in} + (T_{out} - T_{in})\, x / L \qquad (6)$$

The local Nusselt number of the present study was compared with the Nusselt number for fully developed turbulent flow in smooth surfaces correlated by the Dittus-Boelter as :

$$Nu / Nu_{D\text{-}B} = [Q'' \cdot D_e / \{\lambda (T_{wc} - T_b)\}] / (0.023\, Re^{0.8}\, Pr^{0.4}) \qquad (7)$$

$$Nu_{D\text{-}B} = 0.023\, Re^{0.8}\, Pr^{0.4} \qquad (8)$$

where Q'' was surface heat flux supplied by the electrical input.

5. Results and Discussion

5.1 Frictional pressure drop performance

Most of the experimental f data using water, air etc. as a working fluid show negligible effects on the Reynolds number for tubes or channels with surface roughness. Citings of such type of experiments are Webb et al. (1971), Liou et al.(1992), Han et al.(1984) etc. For the rib-roughened surface, rib pitch / height plays predominent role to increase the friction factor for turbulent flows. Figure 7 shows the friction factor predictions from the experimental data with the data of Webb et al. for the k/D_e=0.09, k/D_e=0.04, w/k=1.0 channel geometry and then the k/D=0.02, w/k=0.52 tube geometry with varying p/k ratios. The results show that the friction factor is the highest at p/k=10 both the narrow channel and tube ; then it decreases with increasing or decreasing pitch (p). Frictional pressure drop of the narrow channel causes lower pressure drop than that of the tube.

Figures 8 and 9 compare the friction factor with the smooth surface along with

study. The surface area, A_s was based on the smooth surface area, not including an increase of the area due to ribs. Equation (4) was used for the rib-roughened surface and the smooth surface heat transfer coefficient calculations. The maximum heat loss was taken place at the entry and exit of the test section. The local inner wall temperature (T_w) was at maximum 23℃ in the fully developed region at low Reynolds number and smaller channel heights of the test channel. The local inlet bulk water temperature was at best 15℃ depending on the test conditions. The local bulk water temperature, T_b was calculated assuming a linear water temperature rise along the flow channel and is defined as :

$$T_b = T_{in} + (T_{out} - T_{in})\, x / L \qquad (6)$$

The local Nusselt number of the present study was compared with the Nusselt number for fully developed turbulent flow in smooth surfaces correlated by the Dittus-Boelter as :

$$Nu / Nu_{D\text{-}B} = [Q'' \cdot D_e / \{\lambda (T_{wc} - T_b)\}] / (0.023\, Re^{0.8}\, Pr^{0.4}) \qquad (7)$$

$$Nu_{D\text{-}B} = 0.023\, Re^{0.8}\, Pr^{0.4} \qquad (8)$$

where Q'' was surface heat flux supplied by the electrical input.

5. Results and Discussion

5.1 Frictional pressure drop performance

Most of the experimental f data using water, air etc. as a working fluid show negligible effects on the Reynolds number for tubes or channels with surface roughness. Citings of such type of experiments are Webb et al. (1971), Liou et al.(1992), Han et al.(1984) etc. For the rib-roughened surface, rib pitch / height plays predominent role to increase the friction factor for turbulent flows. Figure 7 shows the friction factor predictions from the experimental data with the data of Webb et al. for the k/D_e=0.09, k/D_e=0.04, w/k=1.0 channel geometry and then the k/D=0.02, w/k=0.52 tube geometry with varying p/k ratios. The results show that the friction factor is the highest at p/k=10 both the narrow channel and tube ; then it decreases with increasing or decreasing pitch (p). Frictional pressure drop of the narrow channel causes lower pressure drop than that of the tube.

Figures 8 and 9 compare the friction factor with the smooth surface along with

prediction and experimental results at different channel heights. The smooth surface friction data agrees well enough with the Blasius correlation. The experimental friction data are underpredicted by about 8 times lower than the prediction at p/k=10, $Re=10^4$ and, H=1.2 mm where experimental results predict 2.4 times higher than the smooth surface. It is seen that the friction factor strongly depends on Re and decreases with increasing Re and p/k ratios. It is obvious that the roughness increases the friction factor with the expense of pressure drop along the flow direction. For the case of a very narrow rectangular channel with one-sided square ribs, the friction factor is expected to be high. The experimental results show very low friction data for the narrow channels which claim further investigation. Since there are almost no data to predict the frictional pressure drop in a very narrow rectangular channel having one-sided repeated-ribs, it is necessary to develop correlations to agree well with the experimental data. Following experimental correlations will be applicable for those narrow channels whose roughness will be one-sided repetitive nature. These correlations are related with the parameter of Re and expressed by the following equations :

$$f = 0.27\ Re^{-0.3} \quad ; \quad p/k=10 \quad , \quad H=1.2\ mm \tag{9}$$

$$f = 0.14\ Re^{-0.25} \quad ; \quad p/k=20 \quad , \quad H=1.2\ mm \tag{10}$$

$$f = 0.054\ Re^{-0.12} \quad ; \quad p/k=10 \quad , \quad H=3.2\ mm \tag{11}$$

$$f = 0.040\ Re^{-0.1} \quad ; \quad p/k=20 \quad , \quad H=3.2\ mm \tag{12}$$

The solid lines passing through the data points are the least-square fits and the average deviations from the measured data are ± 1.2, ± 1.3, ± 3 and $\pm 2\%$ respectively. The correlation [50] which is used to predict the evaluation results is expressed by the following equation :

$$(2 / f)^{1/2} = 2.5 \ln (D/2k) - 3.75 + 0.95\ (p/k)^{0.53} \tag{13}$$

The friction factor affects very small on higher channel heights. It is expected that the friction factor approaches an approximately constant value as the Reynolds number increases which is consistent with the Moody diagram. It can be mentioned that the frictional pressure drop data were taken in the fully developed turbulent flow regime where the location falls under the following categories: x/De=41~66 (TP05) at p/k=10 to x/De=45~74 (TP05) at p/k=20 while H=1.2mm, x/De=17~28 (TP05) at p/k=10 to x/De=18~29 (TP05) at p/k=20 while H=3.2mm for the case of the rib-roughened surface, but for the

smooth surface, x/De=41～67 (TP05), H=1.2mm and x/De=18～30 (TP05), H=2.97mm. These are shown in Figs. (7-9).

5.2 Heat transfer performance

Figures (10 - 15) show the surface temperature distribution along the length of the test section for the smooth and rib-roughened surfaces at different channel heights over a wide range of the Reynolds number. The results show that surface temperature first increases, then it becomes axially unchanging in the fully developed regime and then it decreases. The increasing and decreasing occurs due to not only entrance and exit effects but also heat losses. Surface temperature is higher at lower Reynolds numbers for the smooth cases but opposite for the roughened surfaces. More scattering data are found at higher Reynolds numbers. Figures (16-27) present the surface and bulk temperature distributions along the length of the test section for different channel heights at lower and higher Reynolds numbers. It is seen that at higher Re, the surface temperature is low and the difference between the surface and bulk temperatures is small, because more heat is taken away by the fluid which assists convection mechanism. These figures also reveal that there is a portion of the test section where the surface and bulk temperature distributions are parallel, yielding a uniform value of $(T_w - T_b)$ as expected for constant heat flux. At the inlet and exit of the test section, surface temperature changes remarkably due to entrance and exit effects. The variation of local Nusselt number along the length of the test section for different Re numbers are shown in Figs. (28-33). The Nusselt number is large in the entrance and exit regions. It decreases with increasing axial distance approaching the fully developed values. It is also seen that at higher Re, the curve of the local Nu along the length of the test section is higher whereas at lower Re more uniform Nu data are found.

Figure 34 shows the Nusselt number predictions from the experimental data with the data of Webb et al. for the k/D_e=0.09, k/D_e=0.04, w/k=1.0 channel geometry and then the k/D=0.02, w/k=0.52 tube geometry with varying p/k ratios. The results show that Nu is the highest at p/k=10 both the narrow channel and tube and then it decreases with increasing or decreasing p/k ratios. The solid line passing through the data points of Fig. 34 is the least-square fits which is expressed by the following equation :

$$Nu / Nu_{D\text{-}B} = 5.12\,(p/k)^{-0.252} \qquad (14)$$

The maximum scatter of the data points relative to the least-square line is ± 6.5%. This correlation is much simpler than the Webb et al.'s correlation , fits much closer to the experimental data and basically shows the rib pitch/height effect on heat transfer only. The smooth surface Nu was calculated from the Dittus-Boelter equation. It is also seen from this figure that this correlation will not be applicable to the narrow channel because large variation of heat transfer performance occurs between the tube and narrow channel.

The results would be explained as follows : Since repeated-rib surface is considered as a roughness geometry, it may be also viewed as a problem in boundary layer separation and reattachment. Separation occurs at the rib, forming a widening free shear layer where reattachment occurs down stream from the separation point. A reverse flow boundary layer is originated at the reattachment point. The wall shear stress is zero at the reattachment point and increases from zero in the reverse flow and reattachment regions ; however, the direction of the shear stress is opposite in these regions. As reattachment length is a strong function of rib width(w), rib height(k), and channel height(H), it does not occur for p/k less than about eight. So, the maximum heat transfer coefficient occurs in the vicinity of the reattachment point even though heat transfer coefficients in the separated flow region are larger than those of an undisturbed boundary layer.

From another point of view, the reason can be explained that the reattachment length behind the rib alters slightly with the rib shape as $p/k \geq 10$ and for larger rib spacing, the redeveloping flow beginning at the reattachment point has a larger distance to develop into a thicker boundary layer before the succeeding rib is encountered, hence reduced heat transfer. Figure 35 shows the heat transfer performance for the $k/D_e=0.09$, $w/k=1.0$, $H=1.2$ mm geometry and varying p/k ratios along with prediction. The prediction of heat transfer performance is calculated by the Webb et al.[50] correlation and is expressed by the following equation :

$$St = (f/2) / [1+(f/2)^{1/2} [4.5 (k^+)^{0.28} Pr^{0.57} - 0.95 (p/k)^{0.53}] \quad (15)$$

From this figure, it is seen that the experimental results predict slightly lower heat transfer performance than the prediction and it augments heat transfer about 2-3 times higher than the smooth surface by means of 2.8-4 times frictional pressure drop with $p/k=10$ and $Re=5000 - 10^5$. As shown in Fig. 35,

the solid lines passing through the data points are the least-square fits and can be expressed by the following equations :

$$Nu = 0.416\ Re^{0.57}\ Pr^{0.4} \quad ; \quad p/k = 10 \ , \quad H = 1.2\ mm \qquad (16)$$

$$Nu = 0.434\ Re^{0.55}\ Pr^{0.4} \quad ; \quad p/k = 20 \ , \quad H = 1.2\ mm \qquad (17)$$

The maximum scatters of the data points relative to the least-square lines are ±15 and ±22 % respectively. Figure 36 shows the heat transfer performance for the k/D_e=0.04 , w/k=1.0 and H= 3.2 mm geometry with varying p/k ratios along with prediction and experimental results. The experimental correlations are expressed by the following equations:

$$Nu = 0.384\ Re^{0.6}\ Pr^{0.4} \quad ; \quad p/k = 10 \ , \quad H = 3.2\ mm \qquad (18)$$

$$Nu = 0.365\ Re^{0.6}\ Pr^{0.4} \quad ; \quad p/k = 20 \ , \quad H = 3.2\ mm \qquad (19)$$

It is seen from this figure that higher channel heights do not play any significant role from the view point of heat transfer augmentation. The solid lines passing through the data points are the least-square fits and the maximum deviations are ±10 and ±13% respectively. The heat transfer data were taken in the fully developed region where the location falls under the following categories: x/De=29~71 at p/k=10 to x/De=25~76 at p/k=20 while H=1.2mm and x/De=17 ~26 at p/k=10 to x/De=11~29 at p/k=20 while H=3.2mm for the case of the rib-roughened surface, but for the smooth surface, the position belongs to x/De=42~62 while H=1.2mm to x/De=18~27, H=3.2mm respectively. They are shown in Figs.(34-36).

Such a high heat transfer augmentation performance in a very narrow channel with repeated-ribs would be responsible for creation of turbulence eddies, recirculation and overall increase of surface area. Due to the presence of these, the velocity profiles are relatively flat for the rib-roughened surface compared to the smooth surface. The flatter profiles enhance the transfer of momentum and energy, and hence increase surface friction as well as convection heat transfer rates. The causes for the disagreement of experimental results with the prediction seem to be that the prediction correlations are obtained for those experiments whose parameters are large, experimental conditions are different compared to this experiment. The present experiment is not only non uniform heating but also non symmetric rib-roughened surface from one side. In addition, the heat transfer performance reveals the similar tendency. This discrepancy suggests for

further investigation.

6. Concluding Remarks

The thermal and hydraulic characteristics of the narrow rectangular channels with and without repeated-rib promoters in a single-phase turbulent flow for the target system have been studied experimentally. The friction factor distribution is not consistent with that of the existing works [50]. For the smooth channel flow, both the measured Nusselt number and friction factor agree well with available theoretical correlations. The main findings are :

1. Semi-empirical correlations for friction and heat transfer that are applicable to a very narrow rectangular channel with internally one-sided repeated-rib promoters are presented. These correlations could be useful in the design of the cooling passages between the target plates to remove high heat flux in a high-intensity proton accelerator system.
2. Relative to a smooth surface, the presence of periodic ribs at one-sided walls augments heat transfer 2-3 times higher by means of 2.8-4 times frictional pressure drop for the ranges of Reynolds number, Re=5000 -10^5, dimensionless rib/pitch, p/k=10 and channel height,H=1.2 mm investigated in this current study.
3. The highest heat transfer augmentation which causes the highest frictional pressure drop occurs at p/k=10 compared to other larger or smaller p/k ratios.
4. Friction factor is a strong function of the Reynolds number from the transition to the fully developed regime and is expected to be a asymptotic value at higher Re.
5. Reattachment length is expected to be a strong function of rib width (w), rib height (k), and channel height (H) and be independent of the Reynolds number.
6. Higher channel heights do not play any significant role from the view point of heat transfer augmentation.

Based on the results in this study, it is recommended for further study including the following :

1. Symmetric condition of ribs in the channel with uniform heating and ribs of

various shapes,

2. Non transverse ribs (helix angles other than 90°), which induce a spiral component to the flow,
3. Closer rib spacings corresponding to the separation and recirculation mechanism,
4. Various rib heights to see the effects of its, and
5. Various channel heights to make clear the effectiveness of channel heights.

Acknowledgements

In this study, the authors wish to express their sincere gratitude to Mr. Hideki Aita, Mr. Kenji Sekita, and Mr. Fujisaki for their assistance to carry out the experiments. Without their contributions, the work would not have been possible. Finally with deep sincerity, the authors acknowledge profound indebtness to Dr. M. Z. Hasan, Assoc. professor, Mechanical Engineering Department, Saga University for his guidance, constant encouragement, valuable comments and suggestions.

various shapes,

2. Non transverse ribs (helix angles other than 90°), which induce a spiral component to the flow,
3. Closer rib spacings corresponding to the separation and recirculation mechanism,
4. Various rib heights to see the effects of its, and
5. Various channel heights to make clear the effectiveness of channel heights.

Acknowledgements

In this study, the authors wish to express their sincere gratitude to Mr. Hideki Aita, Mr. Kenji Sekita, and Mr. Fujisaki for their assistance to carry out the experiments. Without their contributions, the work would not have been possible. Finally with deep sincerity, the authors acknowledge profound indebtness to Dr. M. Z. Hasan, Assoc. professor, Mechanical Engineering Department, Saga University for his guidance, constant encouragement, valuable comments and suggestions.

References

[1] Bergles, A.E., Some perspectives on Enhanced Heat Transfer-Second-Generation Heat Transfer Technology, Trans. ASME, J. Heat Transfer, vol.110, pp.1082-1096, 1988

[2] Rabas, T.J., Selection of the Energy-Efficient Enhancement Geometry for Single-Phase Turbulent Flow inside Tubes, in Heat Transfer Equipment Fundamentals, Design, Applications, and Operating Problems, ASME HTD-vol. 108, pp.193-204,1989

[3] Chiou, J.P., Augmentation of Forced Convection Heat Transfer in a Circular Tube Using Spiral Spring Inserts, ASME Paper 83-HT-38. 1983

[4] Zhang, Y.F., Li, F.Y., and Liang, Z.M., Heat Transfer in Spiral-Coiled-Inserted Tubes and its Applications, in Advances in Heat Transfer Augmentation and Mixed Convection, ASME HTD-Vol.169, pp. 31-36,1991

[5] Ravigururajan, T.S., and Bergles, A.E., Study of Water-Side Enhancement for Ocean Thermal Energy Conversion Heat Exchangers, Final Report, College of Engineering, Iowa State University, Ames, 1986

[6] Li, H.M., Ye, K.S., Tan, Y.K., and Deng, S.J., Investigation on Tube-Side Flow Visualization, Friction Factors and Heat Transfer Characteristics of Helical-Ridging Tubes, in Heat Transfer 1982, Proc. 7th Int. Heat Transfer Conf., vol. 3 , pp. 75-80, 1982

[7] Webb, R.L., Turbulent Heat Transfer in Tubes Having Two-Dimensional Roughness, Including the Effect of Prandtl number, Ph. D. thesis, University of Minnesota, Minneapolis, MN, 1969

[8] Nakayama, M., Takahashi, K., and Daikoku, T., Spiral Ribbing to Enhance Single-Phase Heat Transfer inside Tubes, ASME-JAME Thermal Engineering Joint Conf., pp. 365-372, 1983

[9] Yoshitomi, H., Oba, K., and Arima, Y., Heat Transfer and Pressure Drop in Tubes with Embossed Spiral, Thermal and Nuclear Power(in Japanese), vol. 26, pp. 171-182, 1976

[10] Withers, J.G., Tube-Side Heat Transfer and Pressure drop for Tubes Having Helical Internal Ridging with Turbulent/ Transitional Flow of Single-Phase Fluid. Part 1. Single-Helix Ridging, Heat Transfer Eng., vol. 2 no. 1, pp.48-58,1980

[11] Withers, J.G., Tube-Side Heat Transfer and Pressure drop for Tubes Having Helical Internal Ridging with Turbulent/ Transitional Flow of Single-Phase Fluid. Part 2. Multi-Helix Ridging, Heat Transfer Eng., vol. 2 no. 2, pp.43-50,1980

[12] Gee, D.L., and Webb, R.L., Forced Convection Heat Transfer in Helically Rib-Roughened Tubes, Int. J. Heat Mass Transfer, vol.23 , pp. 1127-1136, 1980

[13] Berger, F.P., and Whitehead, A.W., Fluid Flow and Heat Transfer in Tubes with Internal Square Rib Roughening, J. Br. Nuclear Energy Soc., vol. 20, no.2, pp.153-160, pp.605-613, 1977

[14] Migai, V.K., and Bystrov, P.G., Heat Transfer in Profiled Tubes, Thermal Eng., vol. 28, pp. 178-182, 1981

[15] Kalinin, E.K., Drietser, G. A., Yarkho, S. A., and Kusminov, V.A., The Experimental Study of the Heat Transfer Intensification under conditions of Forced One-and Two-Phase Flow In Channels, in Augmentation of Convective Heat and Mass Transfer, ASME Symposium Volume, pp.80-90, 1970

[16] Bolla, G., De Giorgio, G., and Pedrocchi, E., Heat Transfer and Pressure drop Comparison in Tubes with Transverse Ribs and with Twisted Tapes, Energia Nucleare, no.20, pp. 605-613, 1973

[17] Ganeshan, S., and Rao, M.R., Studies on Thermohydraulics of Single and Multi-Start Spirally Corrugated Tubes for Water and Time-Independent Power Law Fluids, Int. J. Heat Mass Transfer, vol. 25, no .7, pp. 1013-1022, 1982

[18] Gupta, R.H., and Rao, M.R., Heat Transfer and Frictional Characteristics of Spirally Enhanced Tubes for Horizontal Condensers, in Advances in Enhanced Heat Transfer, ASME Symposium Volume, pp. 11-21, 1979

[19] Nunner, W., Heat Transfer and Pressure Drop in Rough Tubes, UK Atomic Energy Authority, Harwell, Atomic Energy Research Establishment Lib/ Trans. 786, 1956

[20] Sams, E. W., Heat Transfer and Pressure-Drop Characteristics of Wire-

Coiled Type Turbulence Promotors, TID-7529, Pt. 1, Book 2, Nov. 1957, pp. 390-415, 1956

[21] Kumar, P., and Judd, R.L., Heat Transfer with Coil Wire Turbulence Promotors, Can. J. Chem. Eng., vol. 48, pp. 378-393, 1970

[22] Novozhilov, J.F., and Migai, V.K., Intensifying Convective Heat Transfer within Tubes by Means of Induced Roughness, Teploenergetika, vol. 11, no.6, pp.60-63, 1981

[23] Snyder, P.H., Intensifying Convective Heat Transfer for Moderate Prandtl Number and Reynolds number Flows within Tubes by Means of Wire Coil Type Turbulent Promotors, Westinghouse Research Laboratories Report 72-1E9-RELIQ-R1, 1972

[24] Sethumadhavan, R., and Rao, M. R., Turbulent Flow Heat Transfer and Fluid Friction in Helical-Wire-Coil-Inserted Tubes, Int.J. Heat Mass Transfer, vol. 26, pp. 1833-1845, 1983

[25] Molloy,J., Rough Tube Friction Factors and Heat Transfer Coefficients in Laminar and Transition Flow, UKAEA AERE-R5415, 1967

[26] Ravigurujan, T.S., General Correlations for pressure Drop and Heat Transfer for Single-Phase Turbulent Flow in Ribbed Tubes, Ph. D. thesis, Iowa State University, Ames, 1986

[27] Mehta, M.H., and Rao, M.R., Heat Transfer and Frictional Characteristics of Spirally Enhanced Tubes for Horizontal Condensers, in Advances in Enhanced Heat Transfer, ASME Symposium Volume, pp. 11-22, 1979

[28] Cunningham, J., and Milne, H.N., The Effect of Helix Angle on the Performance of Rope Tubes, Proc. Sixth Int. Heat Transfer Conf., vol. 2 pp. 601-605, 1978

[29] Mendes, P.R.S., and Mauricio, M.H.P., Heat Transfer, Pressure Drop, and Enhancement Characteristics of the Turbulent through Internally Ribbed Tubes, ASME HTD Vol. 82, pp. 15-22, 1987

[30] Yampolsky, J.S., Libby, P.A., Launder, B.E., and LaRue, J.C., 1984, Fluid Mechanics and Heat Transfer Spiral Fluted Tubing, Final Report, GA Technologies Report GA-A17833, 1984

[31] Scaggs, W.F., Taylor, P. R., and Coleman, H.W., Measurement and Prediction of Rough Wall Effects of Friction Factor in Turbulent Pipe Flow, Report TFD-88-1, Mississippi State University, 1988

[32] Newson, I.H., and Hodgson, T.D., The Development of Enhanced Heat Transfer Condenser Tubing, Desalination, Vol. 14, pp. 291-323, 1974

[33] Sutherland, W.A., and Miller, C.W., Heat Transfer to Superheater Steam-I, Improved Performance with Turbulent Promoters, USAEC Report, GEAP-4749, 1964

[34] Smith, J. W., and R.A. Gowen, 1965, Heat Transfer Efficiency in Rough Pipes at High Prandtl Number, AIChE J., vol. 11, pp. 941-943, 1965

[35] Takahashi, K., Kayama, W., and Kuwahara, H., Enhancement of Forced Convective Heat Transfer in Tubes Having Three-Dimensional Spiral Ribs, Trans. JSME, vol. 51, pp. 350-355, 1985

[36] Obot, N.T., and Esen, E.B., Heat Transfer and Pressure Drop for air Flow through Enhanced Passages, Report DOE/CE/90029-8, Fluid Mechanics, Heat, and Mass Transfer Laboratory Report, FHMT Report 007, Clarkson University, Potsdam, NY, 1992

[37] Kidd, G.I., The Hear Transfer and pressure-Drop Characteristics of Gas Flow inside Spirally Corrugated Tubes, J. Heat Transfer, vol. 92, pp. 513-519, 1970

[38] Arman, B., and Rabas, T.J., Influence of Discrete and Wavy Disruption Shapes on the Performance of Enhanced Tubes, ASME/ AICh E Natl. Heat Transfer Conf. Atlanta, GA, 1993

[39] Bejan, A., 1989, Convective Heat Transfer, John Wiley & Sons, New York .

[40] Berger F.P. and Hau K.-F, F.-L., 1979, Local Mass / Heat Transfer Distribution on surfaces Roughened with Small Square Ribs, Int. J. Heat Mass Transfer, Vol. 22, pp. 1645 - 1656.

[41] James, C. A., Hodge, B.K., and Taylor, P.R., 1993, A Discrete Element Method for The Prediction of Friction and Heat Transfer Characteristics of Fully-Developed Turbulent flow in Tubes with Rib-roughness, HTD - Vol. 239, Turbulent Enhanced Heat Transfer ASME .

[42] James, C. A., Hodge, B.K., and Taylor, P.R., 1993, A Discrete Element Predictive Method for Two-Dimensional Rib Roughness in Fully-Developed Turbulent pipe flow, FED - Vol. 150, Individual papers in Fluids Engineering, ASME .

[43] Han, J.C., Glicksman, L.R., and Rohsenow, W.M.,1978, An Investigation

of Heat Transfer and Friction for Rib- Roughened surfaces, Int. J. Heat Mass Transfer, Vol. 21, pp. 1143 - 1156.

[44] Han, J.C., 1984, Heat Transfer and Friction factor in Channels with Two Opposite Rib-Roughened Walls, Transactions of The ASME, Vol. 10 pp.774 - 781.

[45] Han, J.C., Park, J.S., and Lei, C.K., 1985, Heat Transfer Enhancement in Channels with Turbulence Promoters, Transactions of The ASME, Vol. 107, pp. 628- 635.

[46] IPNS Upgrade, 1995 : A Feasibility Study, ANL-95/13, Argonne National Laboratory, April.

[47] Liou, -M.T. and Hwang,-J.J., 1993, Effect of Ridge Shapes on Turbulent Heat Transfer and Friction in a Rectangular Channel, Int. J. Heat Mass Transfer, Vol. 36, No.4 pp. 931 - 940.

[48] Liou, -M.T. and Hwang,-J.J., 1992, Turbulent Heat Transfer Augmentation and Friction in Periodic fully Developed Channel Flows, Transaction of The ASME, Vol.114, pp. 56 - 64.

[49] Rohsenow, W. M and Hartnett, J.P, 1973, Hand book of Heat Transfer, McGraw-Hill, New York.

[50] Webb, R.L., Eckert, E.R.G., and Goldstein, R.J., 1971, Heat Transfer and Friction in Tubes With Repeated-Rib Roughness, Int. J. Heat Mass Transfer, Vol. 14, pp. 601- 617.

[51] Zhang, Y.M. Gu, W.Z., and Han, J.C., 1994, Heat Transfer and Friction in Rectangular Channels with Ribbed or Ribbed-Grooved Walls, Transactions of The ASME, Vol. 116, pp. 58 - 65

[52] Islam. M.S., 1995, Study of Heat Transfer Performance of a Tube having Internal Fins, Undergraduate thesis, Bangladesh University of Engineering and Technology.

[53] Islam, M.S., Hino, R., Haga, K., Monde, M., and Sudo, Y., Study on Heat Transfer Augmentation in Rib-Roughened Narrow Channels, JSME Conference, Nagoya, March, 7-8, 1997, pp. 269-270.

[54] Islam, M.S., Hino, R., Haga, K., Monde, M., and Sudo, Y., Investigation on Heat Transfer Augmentation for High Heat Flux Removal in Rib-Roughened Narrow Channels, Report, Japan Atomic Energy Research Institute, JAERI-Tech, 97-008. 1997

Nomenclature

a_1, a_2, a_3	empirical constants
b_1, b_2, b_3	empirical constants
A_x	flow cross sectional area, m^2
A_s	surface area , m^2
C_p	specific heat, J/kg℃
D_e	equivalent diameter, $D_e = 4WH / 2(W+H)$, m
f	roughened friction factor
g	acceleration due to gravity , m/s^2
h	forced convection heat transfer coefficient , W / m^2℃
H	channel height , m
k	rib height , m
K	geometry constant
k^+	roughness Reynolds number, $k^+ = (k/D_e) Re (f/2)^{½}$
L	channel length , m
Nu	Nusselt number, $Nu = hD_e / \lambda$
p	rib spacing , m
ΔP	pressure difference , N / m^2 [refer to eq.(1)]
Pr	Prandtl number, $Pr = C_p \mu / \lambda$
q''	heat flux , W / m^2
Re	Reynolds number, $Re = D_e u_m / \nu$
St	Stanton number, $St = Nu / Pr Re$
T_b	bulk mean temperature, ℃
T_w,	wall temperature , ℃
u_m	average fluid velocity , m/s
w	rib width , m
W	width of the channel , m
x	local distance along the axial direction , m

Greek symbol

μ	dynamic viscosity , kg/m.s
ν	kinematic viscosity , m^2/s
ρ	density , kg/m^3
δ	copper material thickness, m
λ	thermal conductivity , W/m℃
Δ	increment

Subscripts

b	bulk
m	mean
o	smooth surface
wc	corrected wall
D -B	Dittus-Boelter

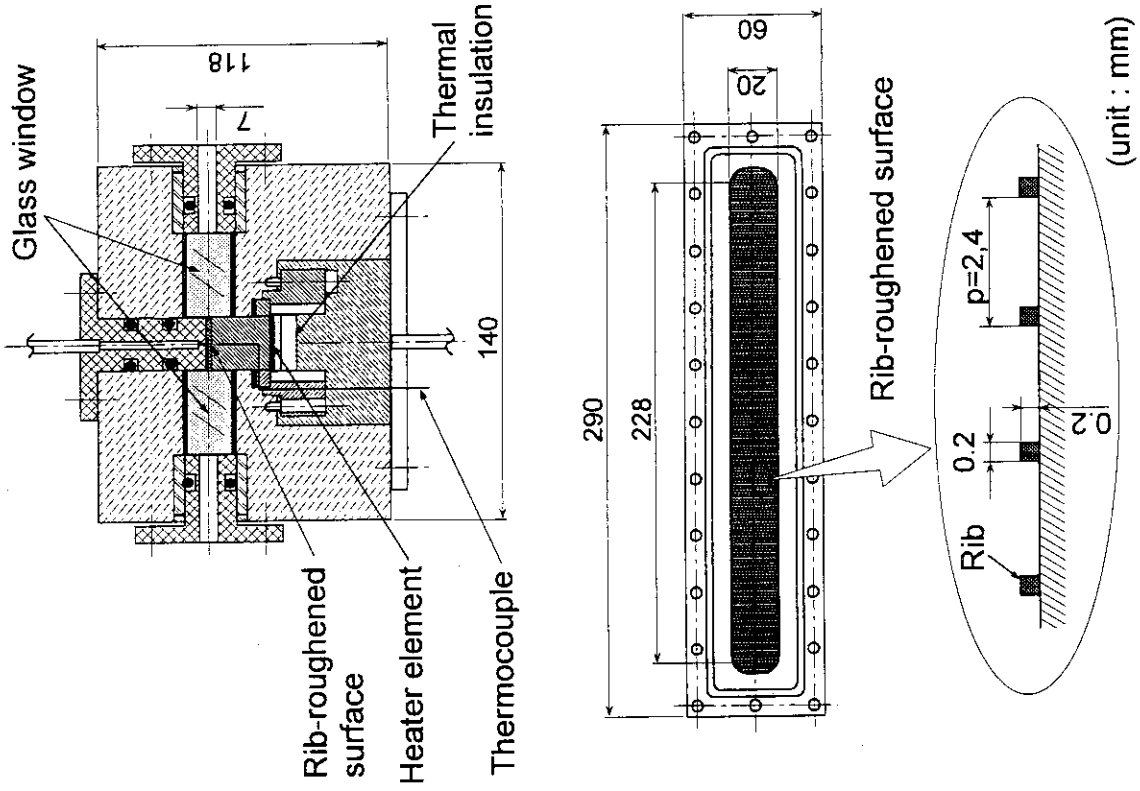

Fig.2 Schematic drawing of test section

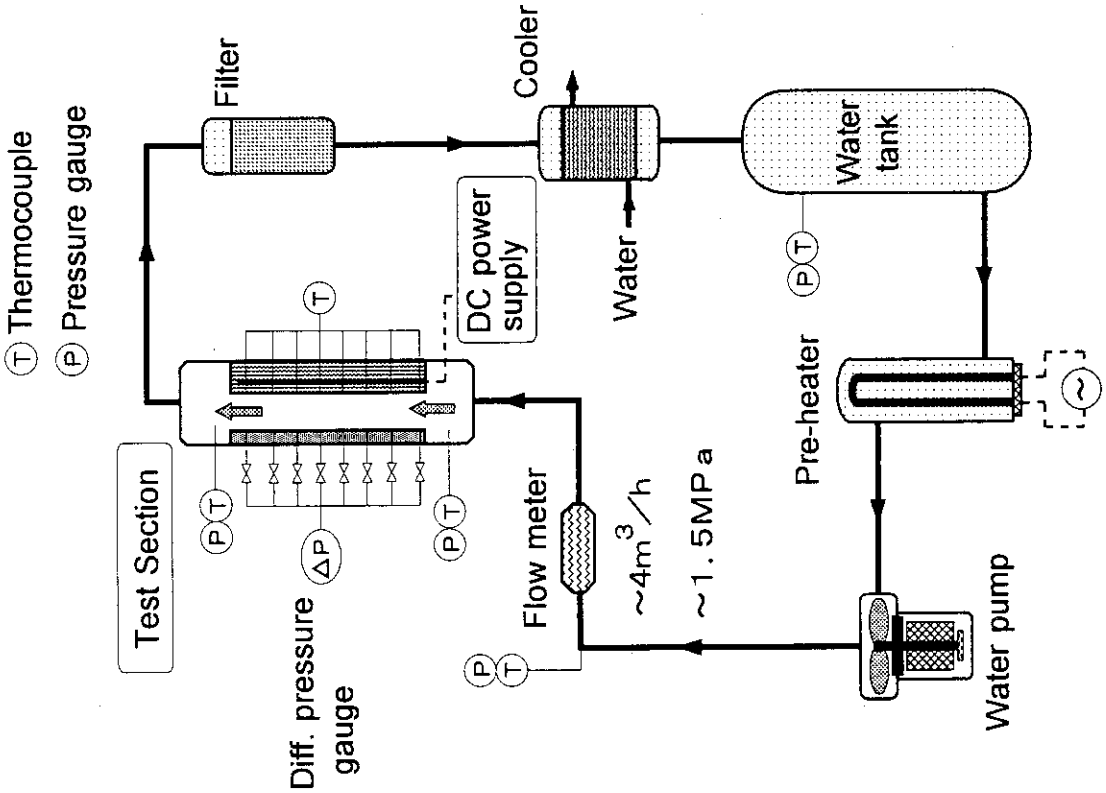

Fig.1 Schematic diagram of test apparatus

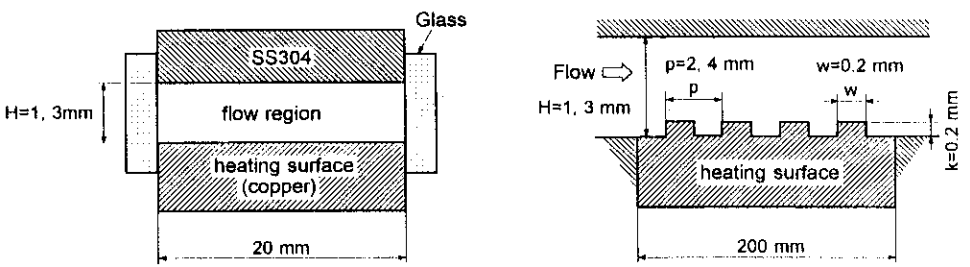

Cross section of flow channel　　Flow channel with rib-roughened surface

Fig.3　Schematic drawing of cross section of flow channel with rib-roughened surface

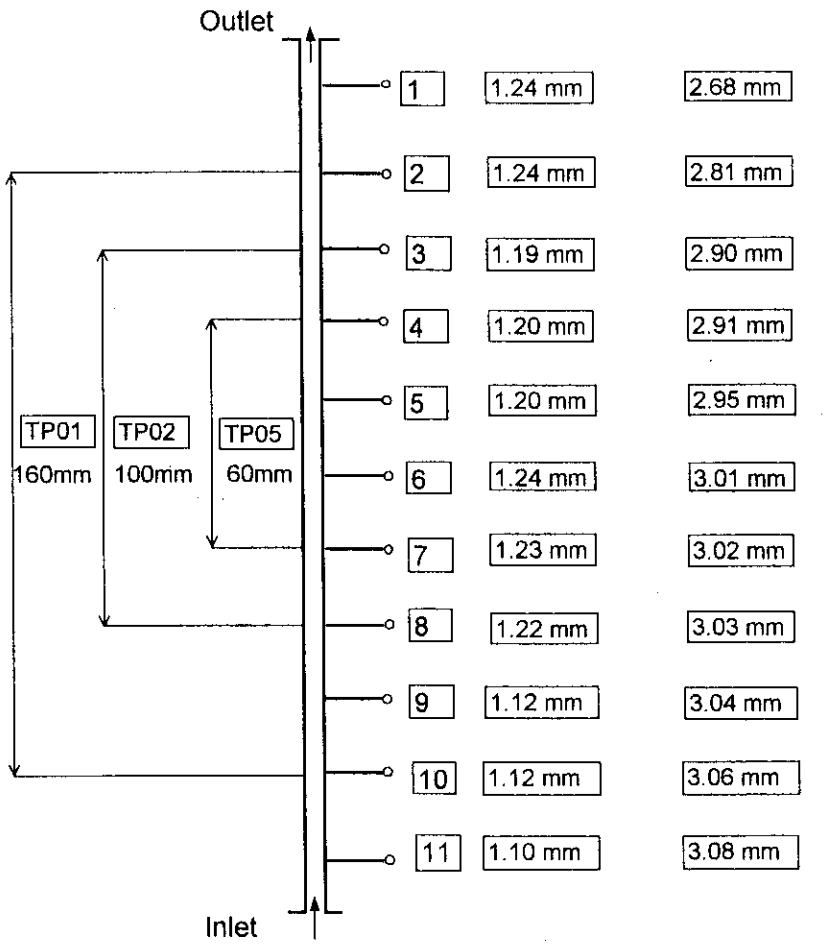

Fig. 4　Local channel height for two different channels (Smooth)

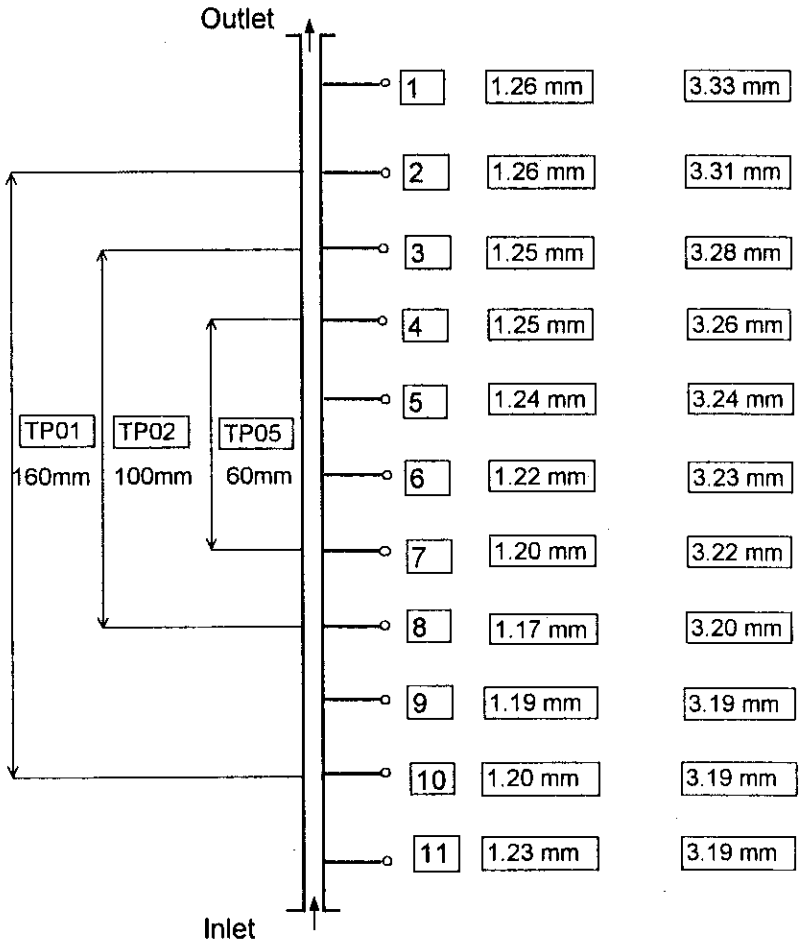

Fig. 5 Local channel height for two different channels
(Roughened surface, p= 2 mm)

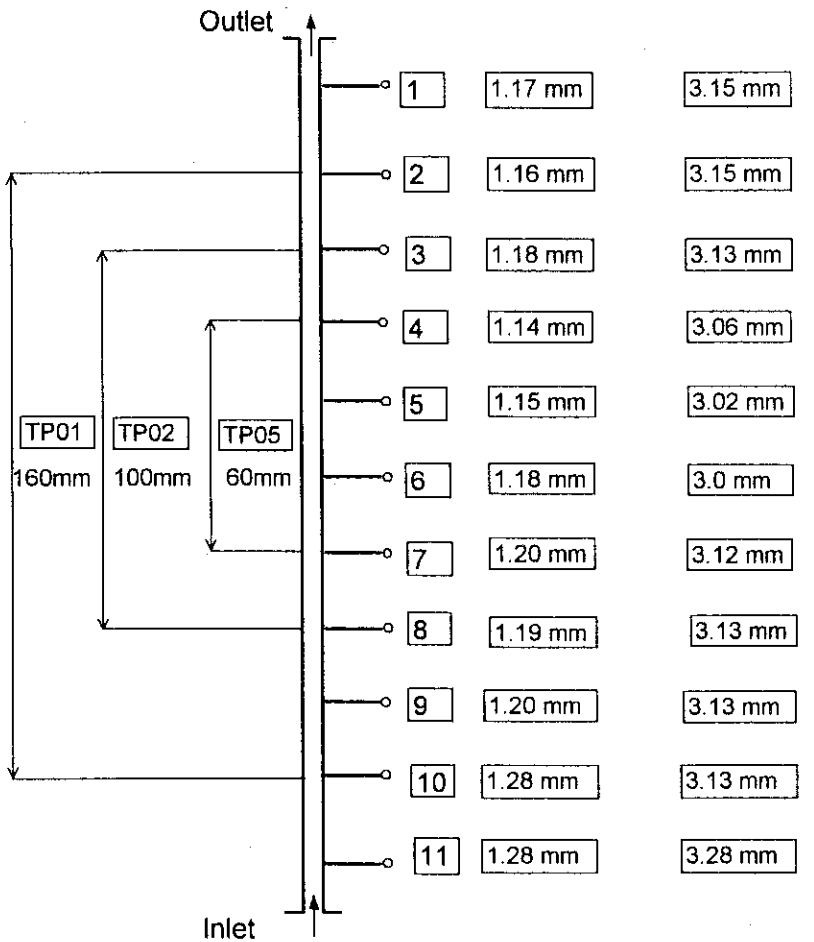

Fig. 6 Local channel height for two different channels
(Roughened surface, p= 4 mm)

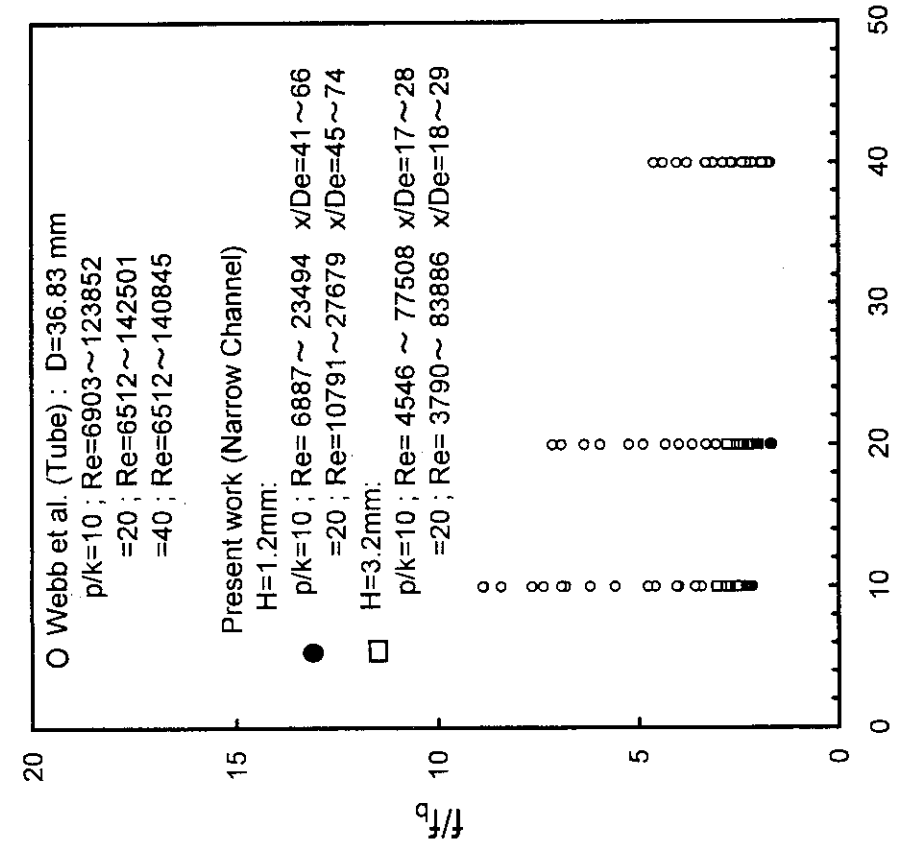

Fig. 7 Friction factor predictions from the experimental data with the data of Webb et al. for the k/D_e=0.09, k/D_e= 0.04, w/k=1.0 channel geomerty and for the k/D=0.02, w/k=0.52 tube geomerty with varying p/k ratios.

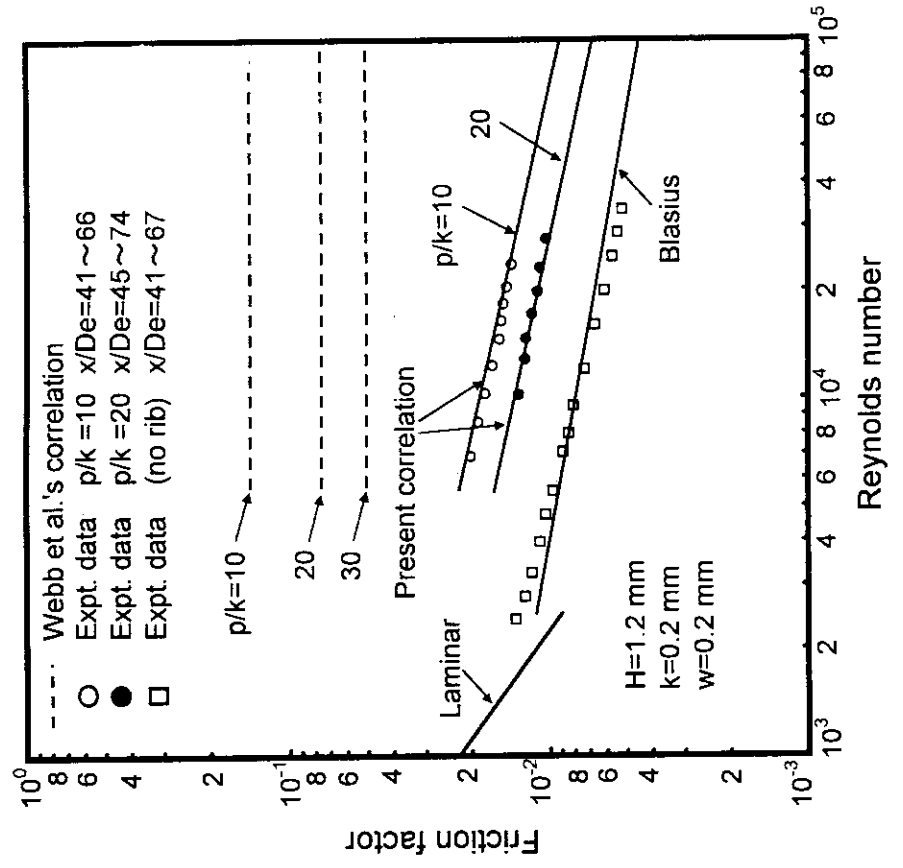

Fig. 8 Comparison of friction correlations with Webb et al.

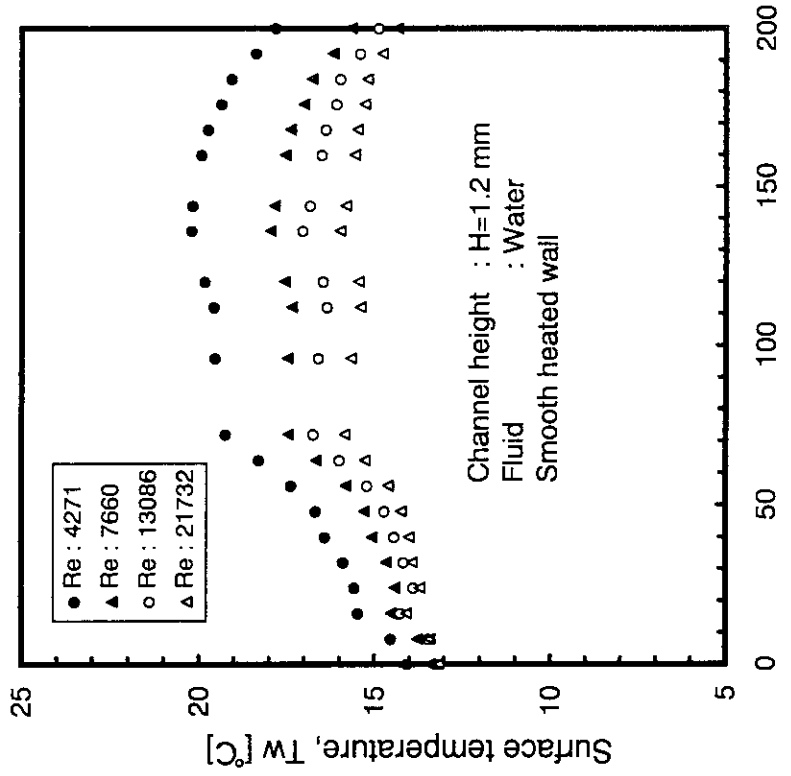

Fig. 10 Local surface temperature distributions along the flow direction of the test section.

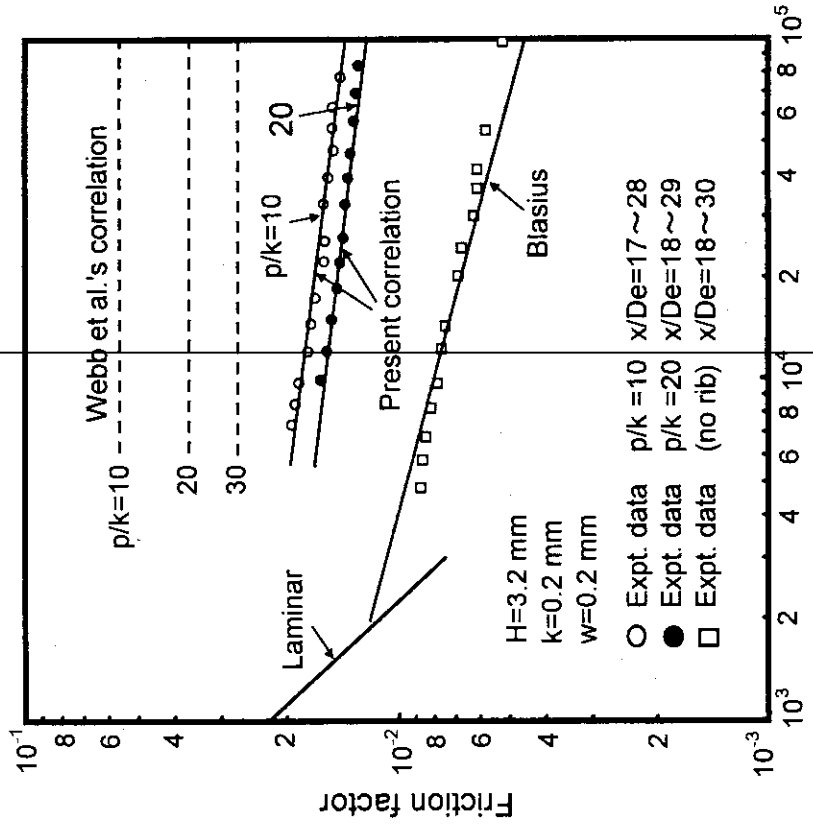

Fig. 9 Comparison of friction correlations with Webb et al.

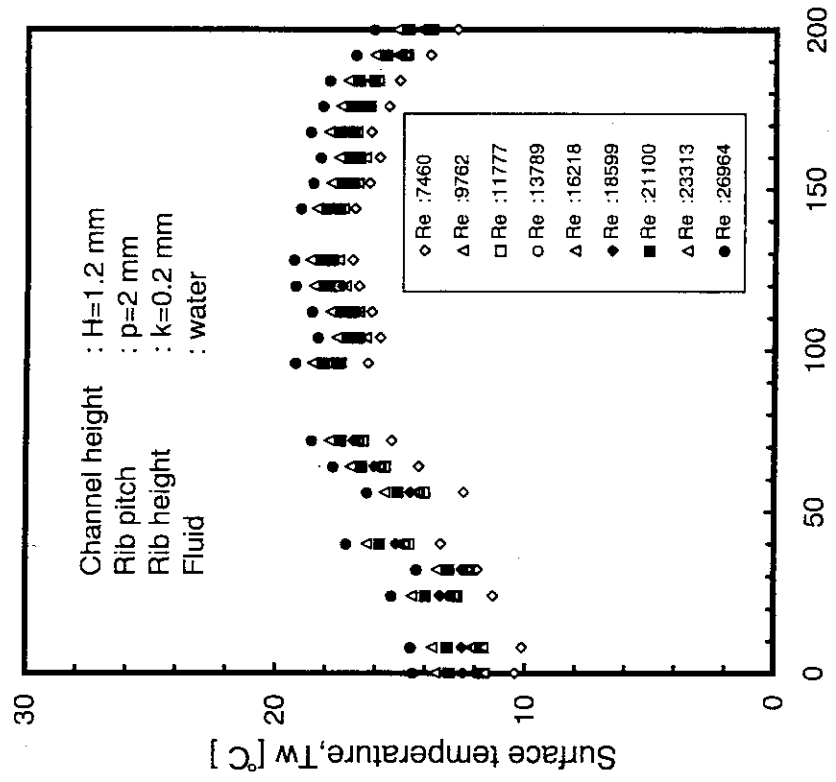

Fig. 12 Local surface temperature distributions along the flow direction of the test section.

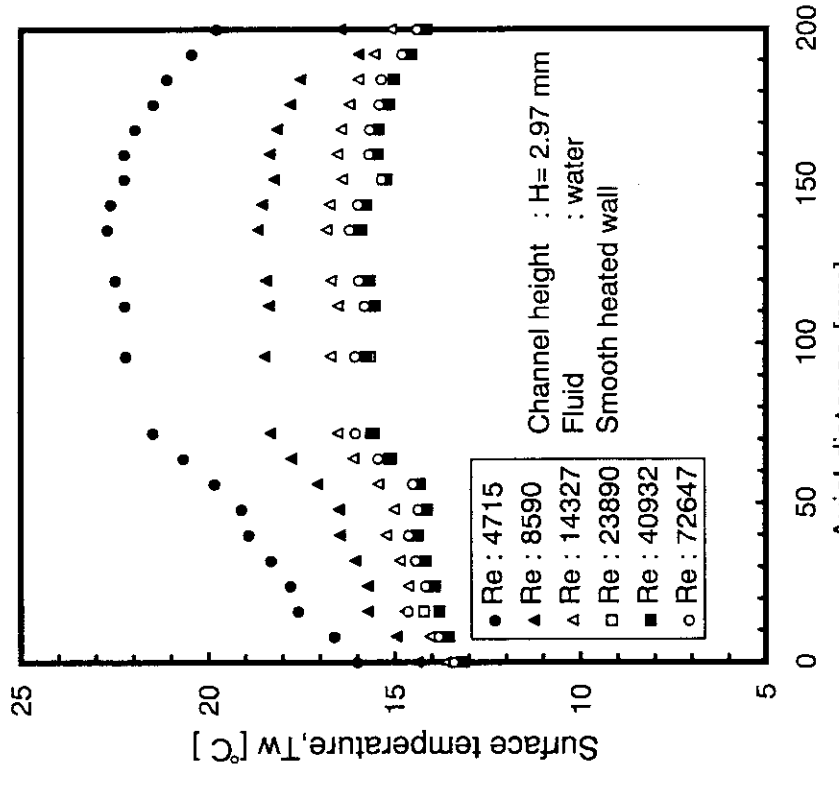

Fig. 11 Local surface temperature distributions along the flow direction of the test section.

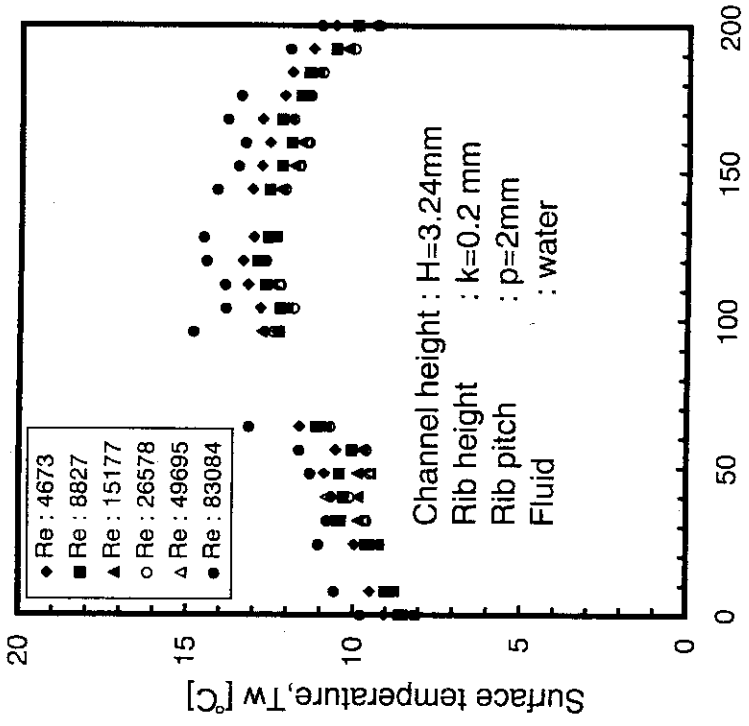

Fig. 14 Local surface temperature distributions along the flow direction of the test section.

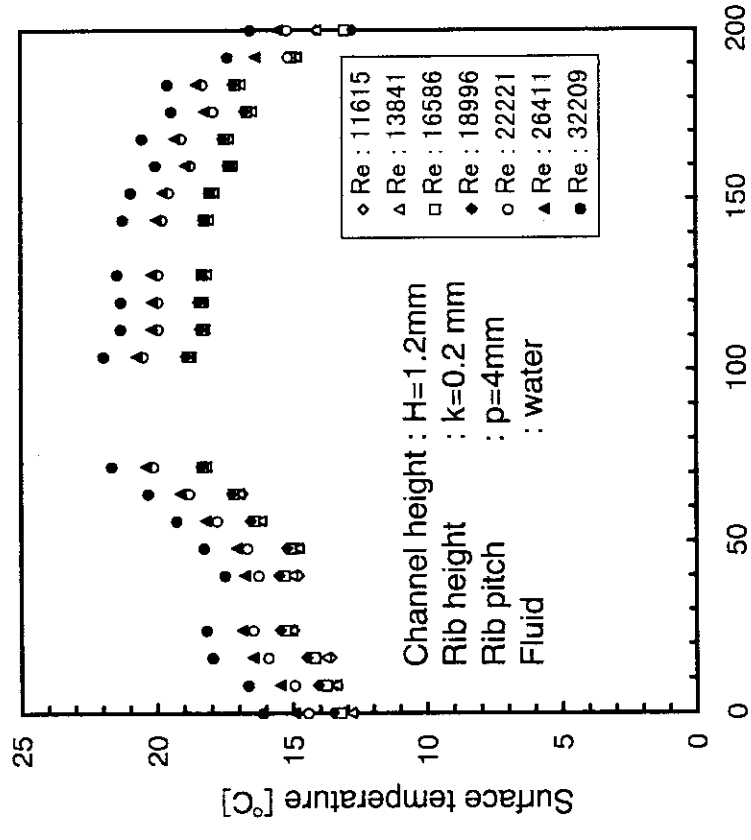

Fig. 13 Local surface temperature distributions along the flow direction of the test section.

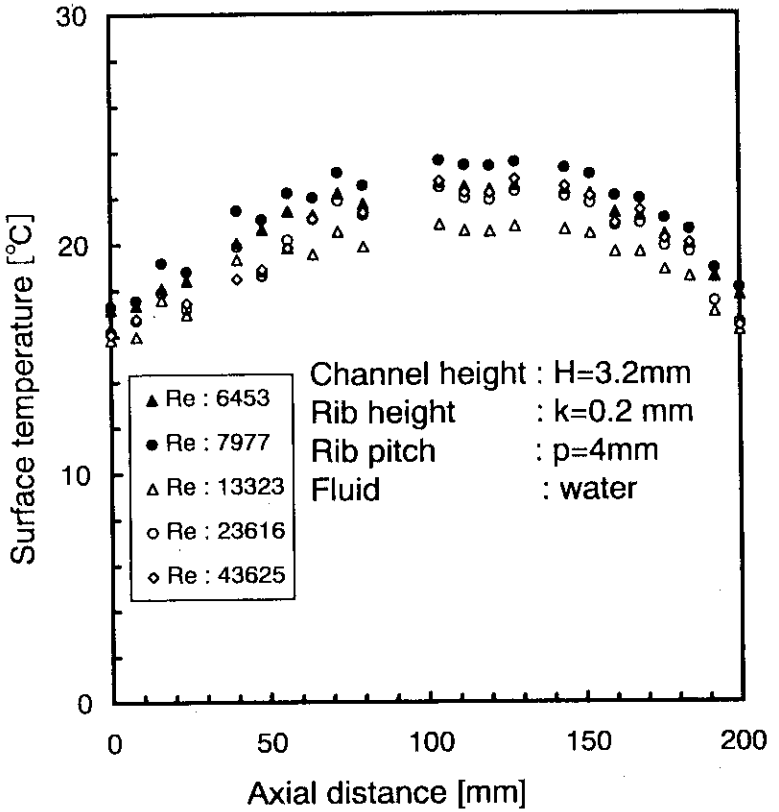

Fig. 15 Local surface temperature distributions along the flow direction of the test section.

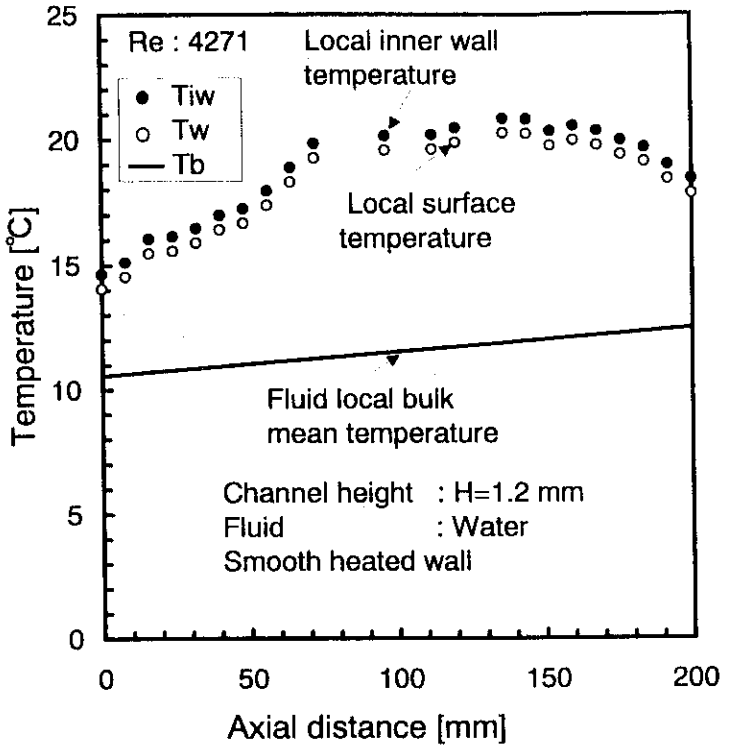

Fig. 16 Local surface and bulk temperature distributions along the flow direction of the test section.

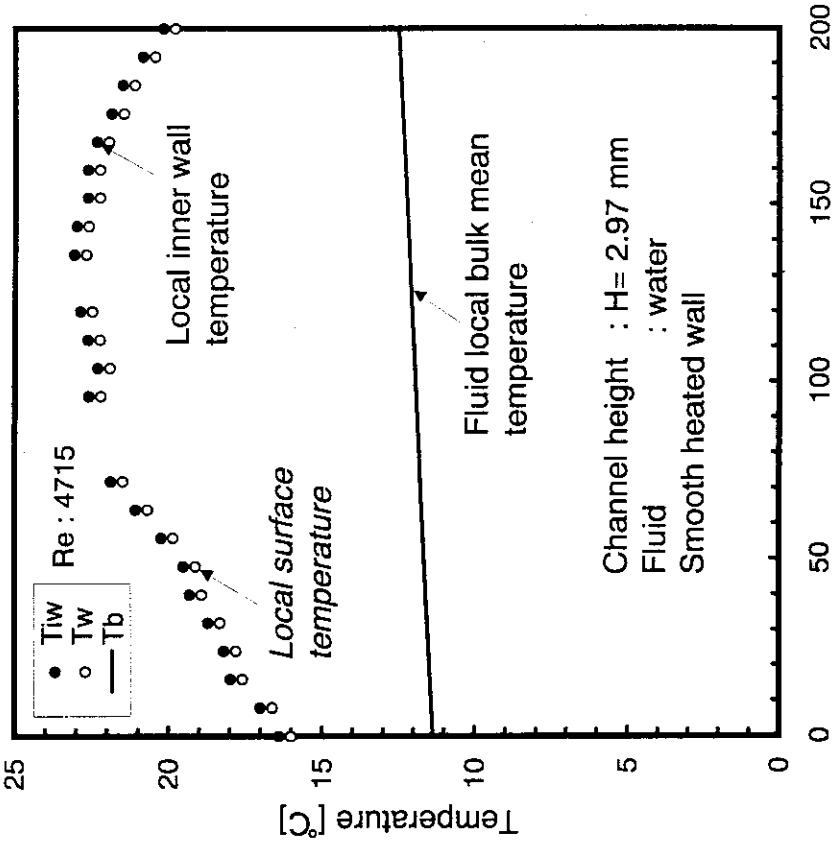

Fig. 18 Local surface and bulk temperature distributions along the flow direction of the test section.

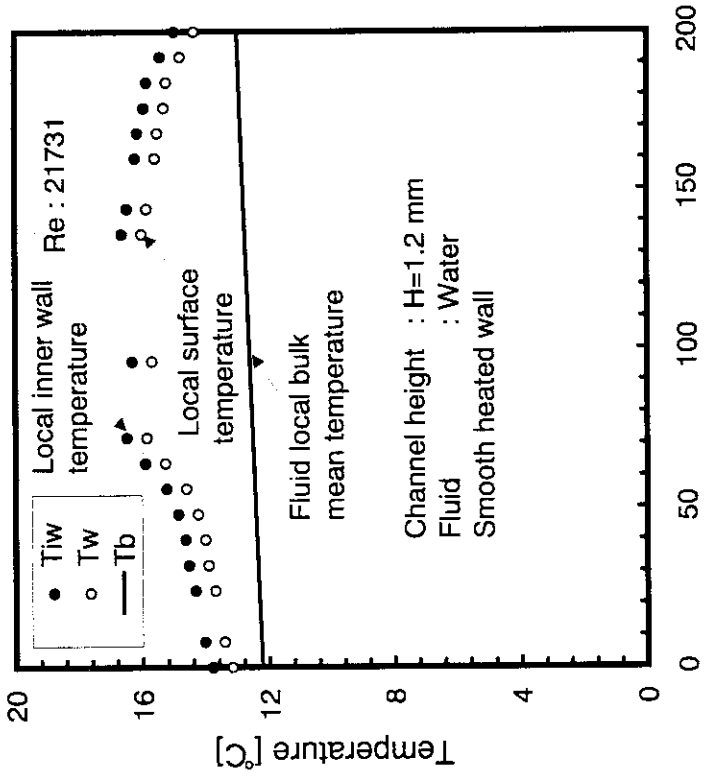

Fig. 17 Local surface and bulk temperature distributions along the flow direction of the test section.

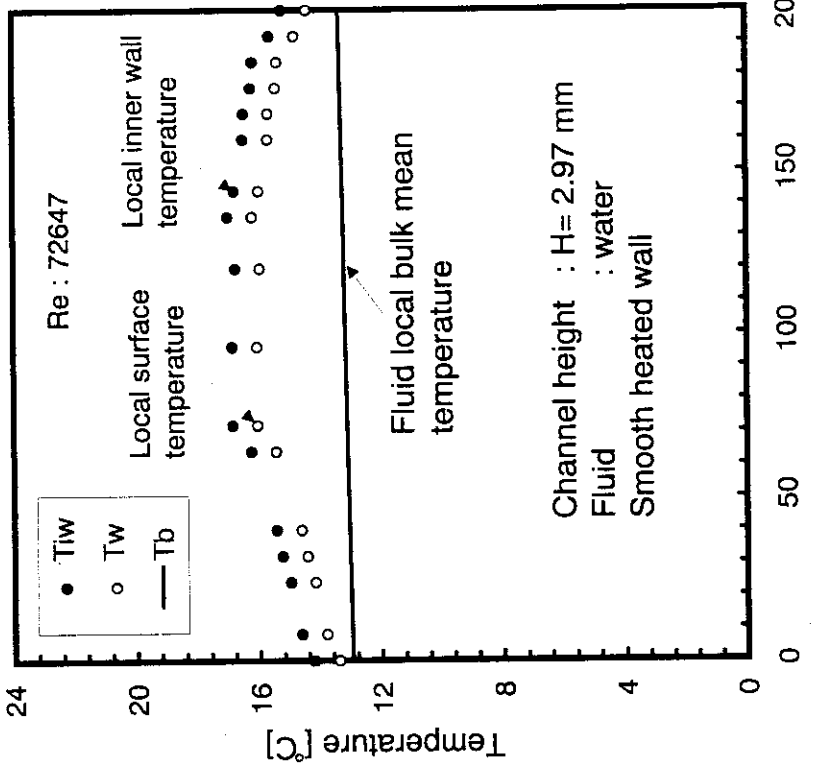

Fig. 19 Local surface and bulk temperature distributions along the flow direction of the test section.

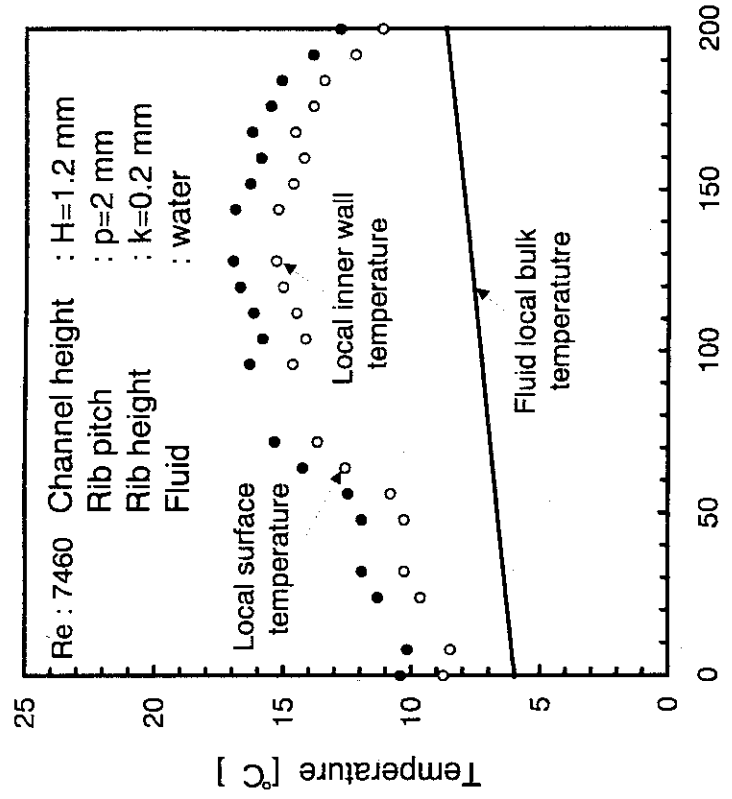

Fig. 20 Local surface and bulk temperature distributions along the flow direction of the test section.

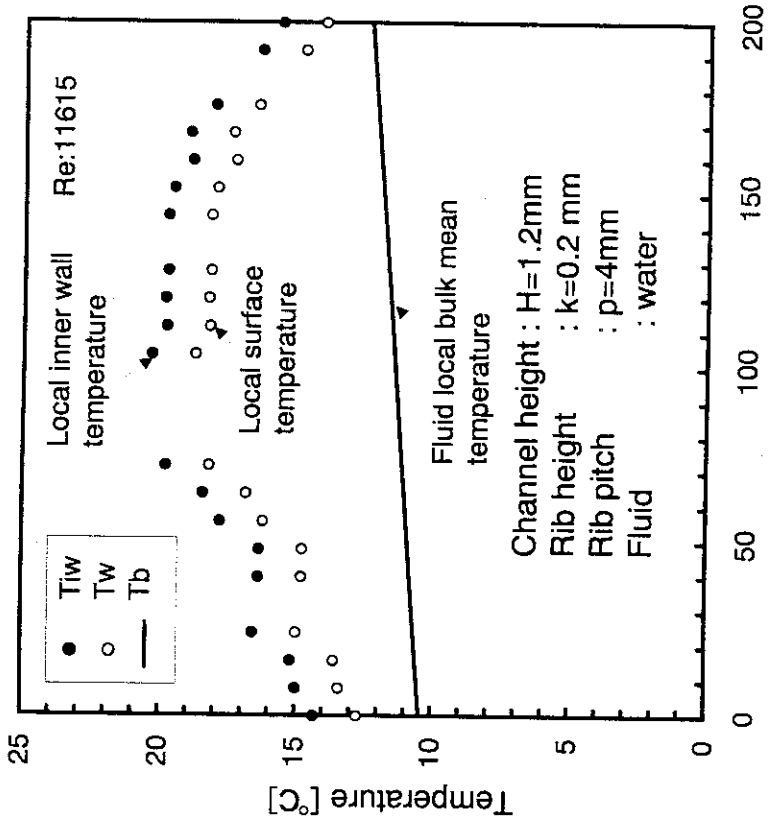

Fig. 22 Local surface and bulk temperature distributions along the flow direction of the test section.

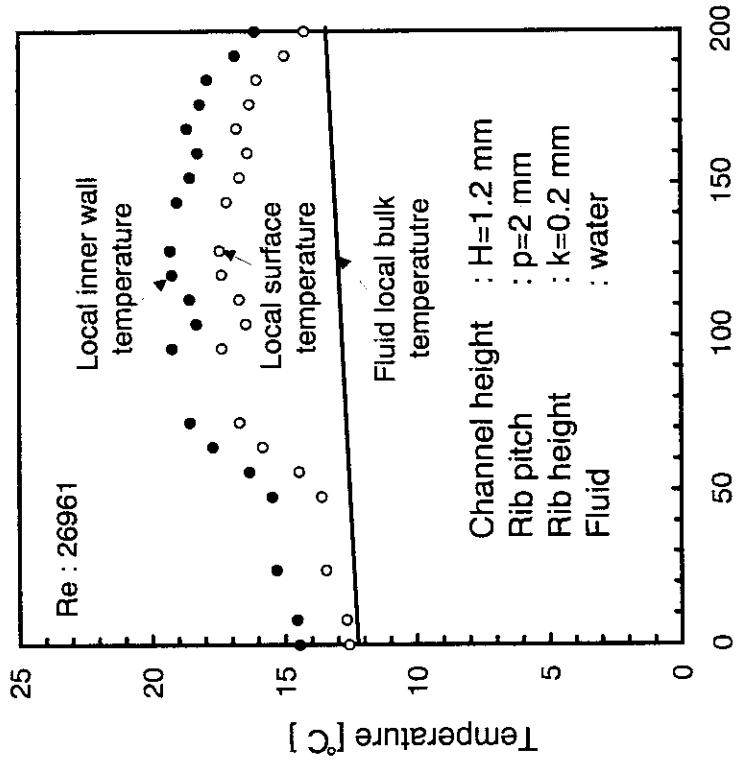

Fig. 21 Local surface and bulk temperature distributions along the flow direction of the test section.

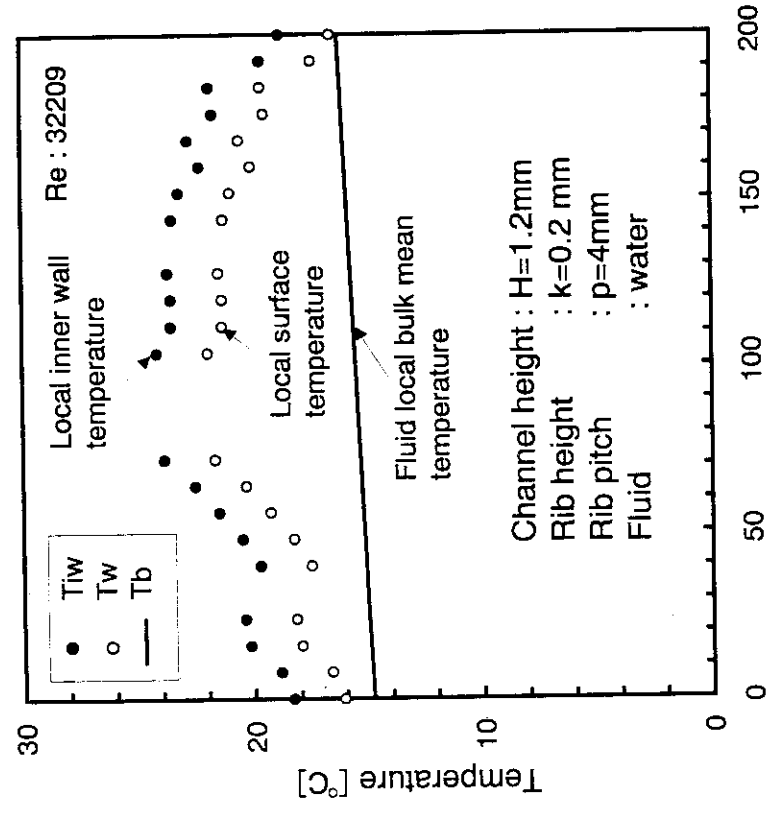

Fig. 23 Local surface and bulk temperature distributions along the flow direction of the test section.

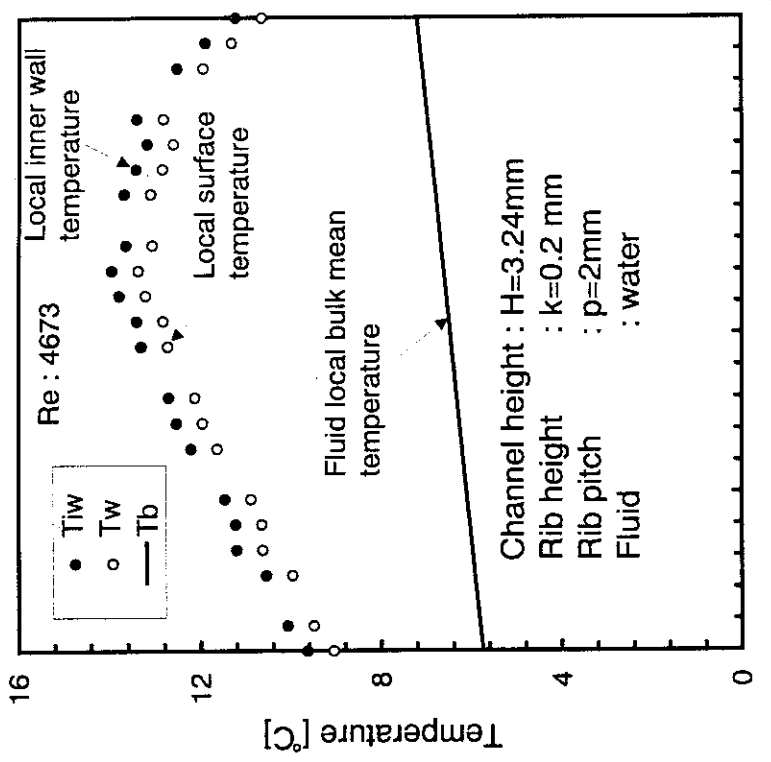

Fig. 24 Local surface and bulk temperature distributions along the flow direction of the test section.

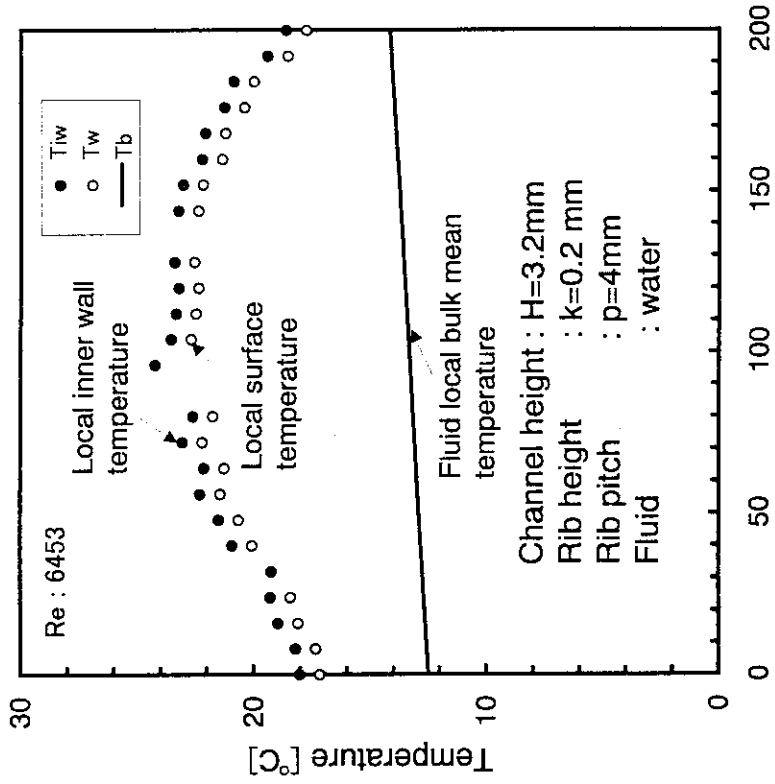

Fig. 26 Local surface and bulk temperature distributions along the flow direction of the test section.

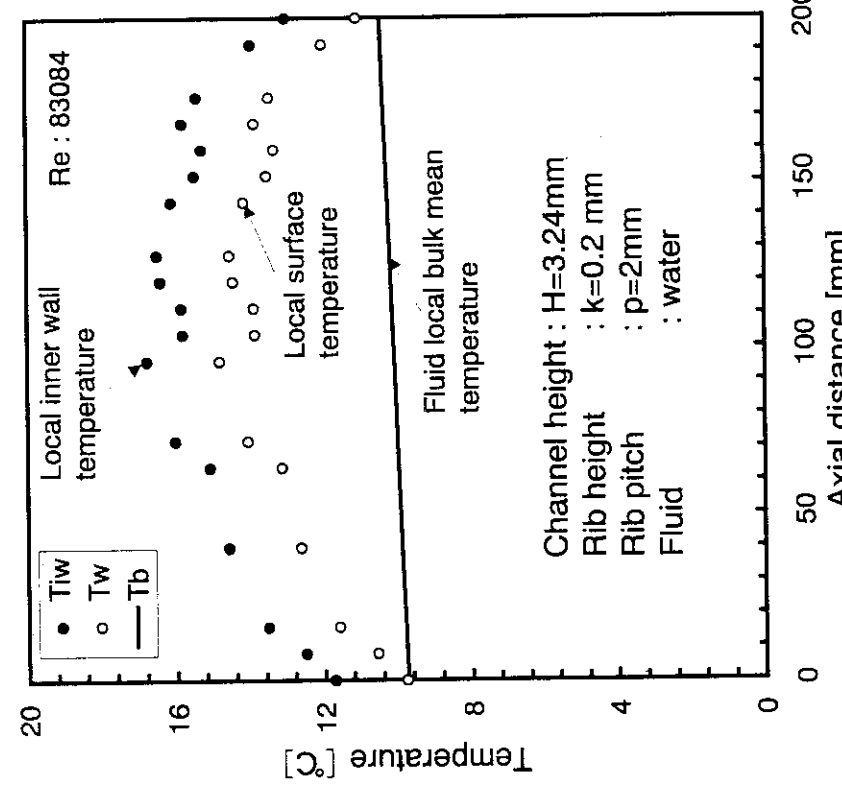

Fig. 25 Local surface and bulk temperature distributions along the flow direction of the test section.

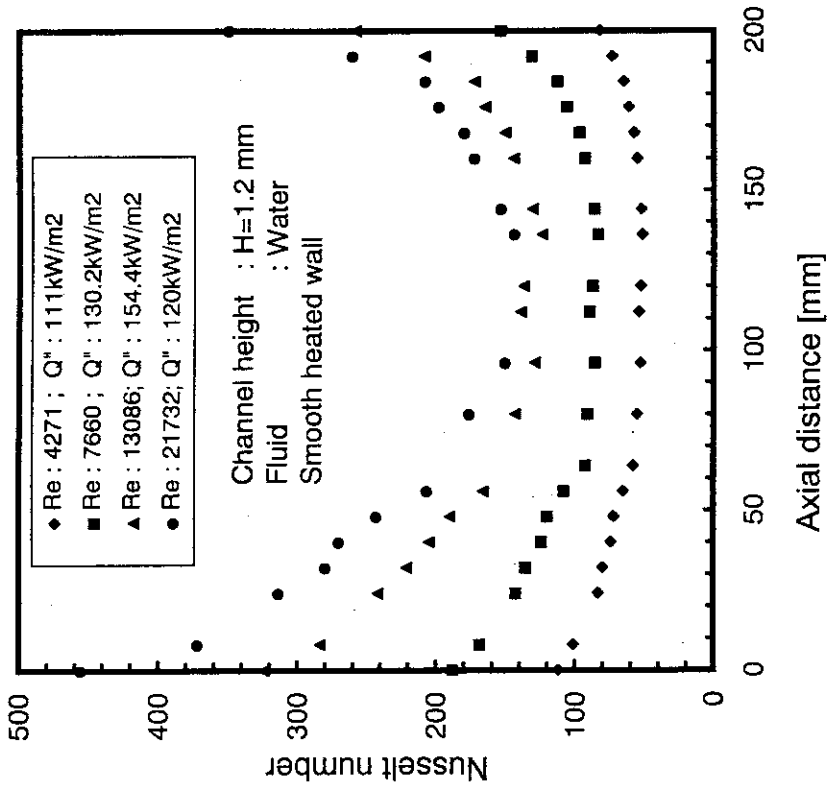

Fig. 28 Local Nusselt number distributions along the flow direction of the test section.

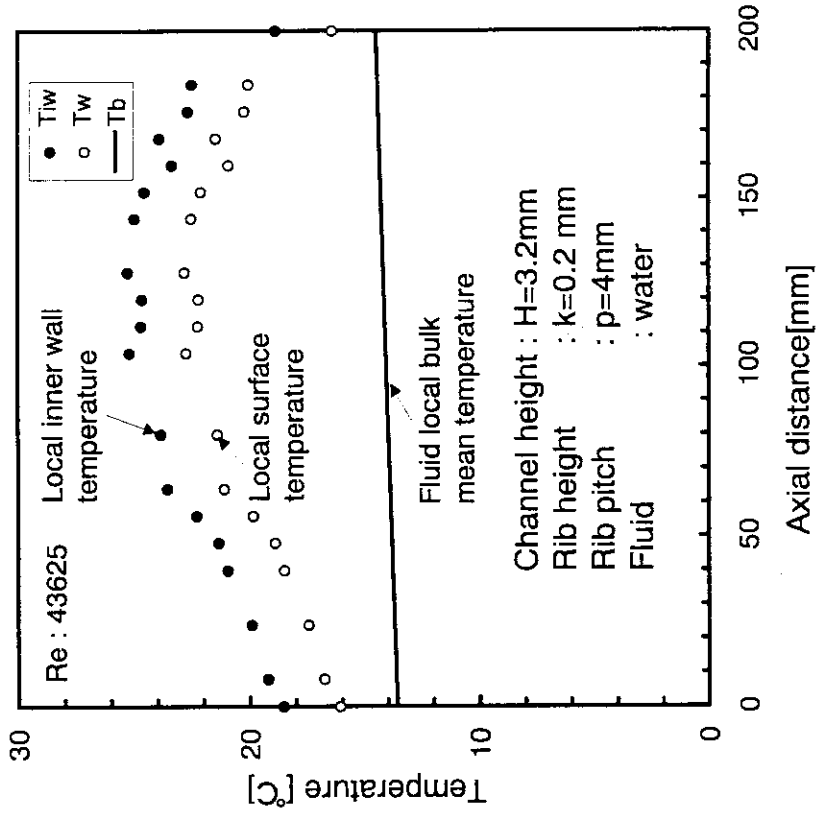

Fig. 27 Local surface and bulk temperature distributions along the flow direction of the test section.

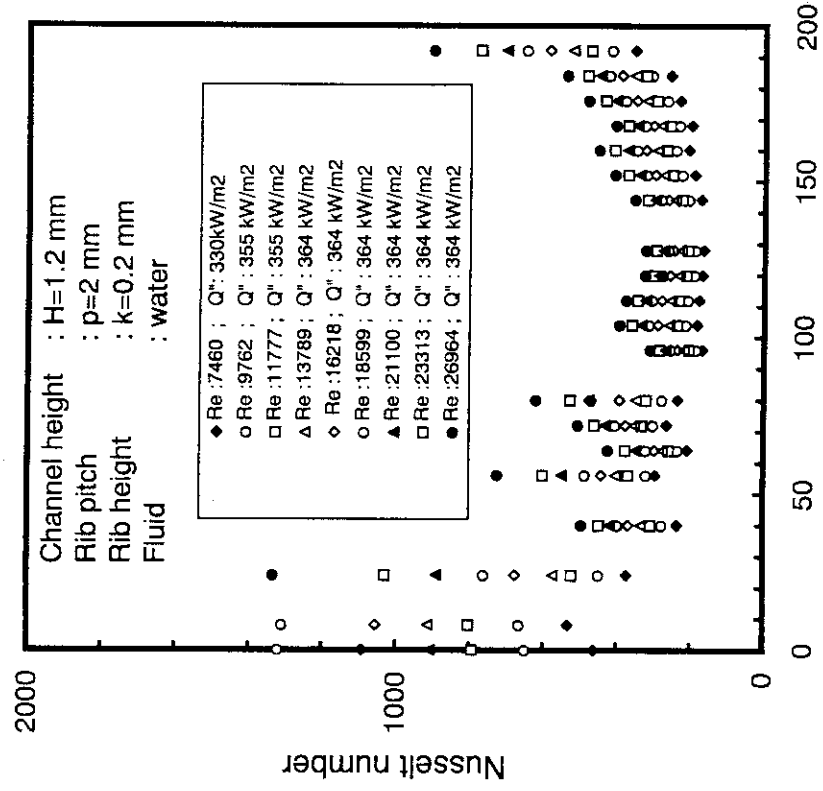

Fig. 30 Local Nusselt number distributions along the flow direction of the test section.

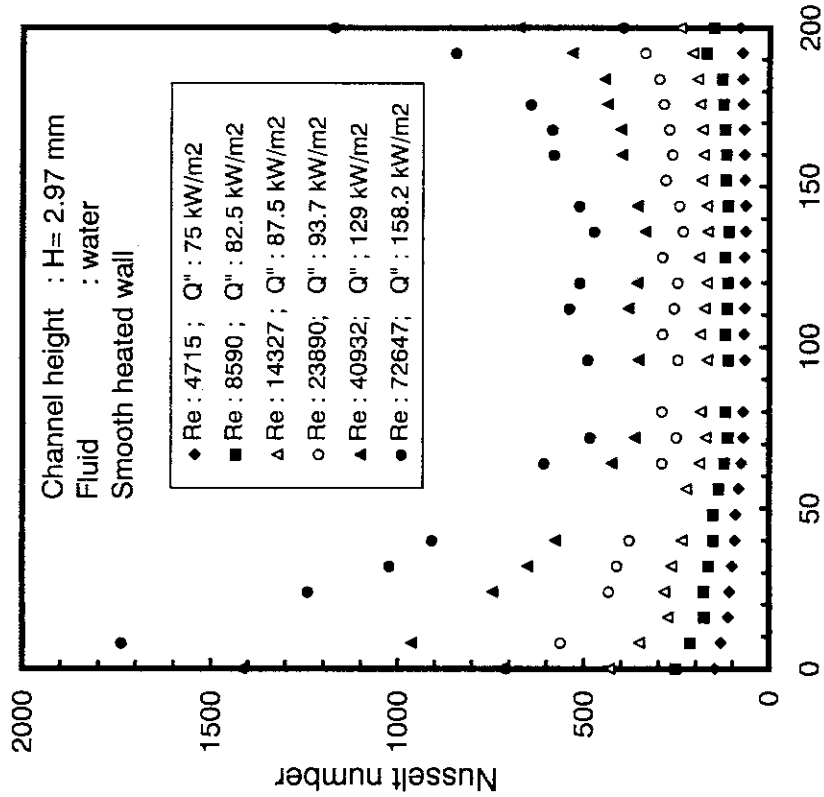

Fig. 29 Local Nusselt number distributions along the flow direction of the test section.

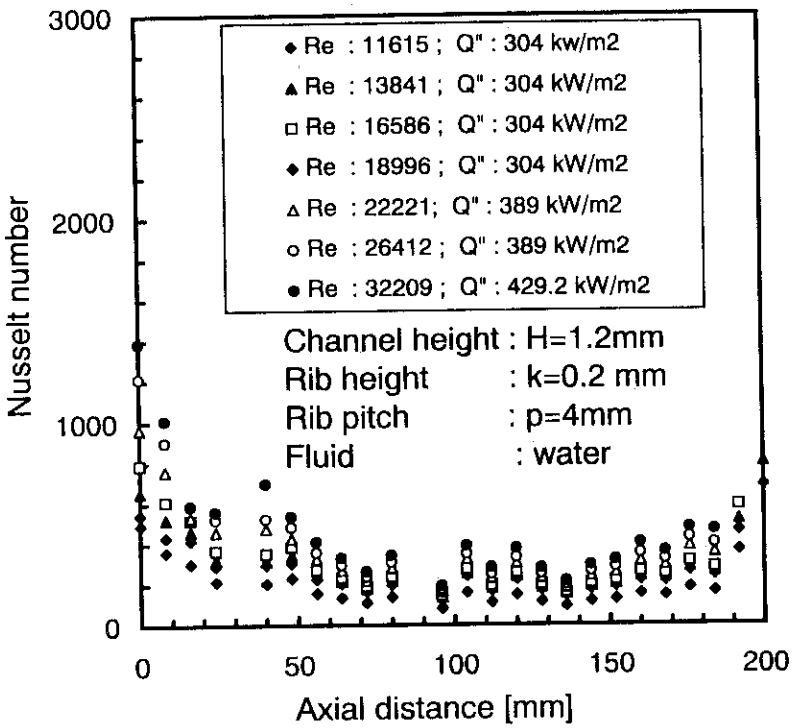

Fig. 31 Local Nusselt number distributions along the flow direction of the test section.

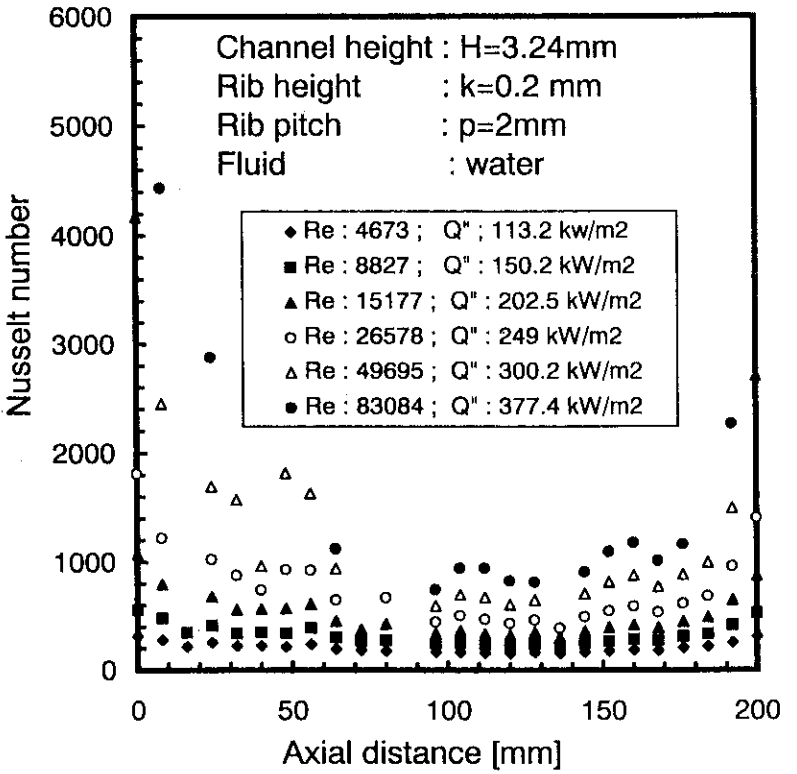

Fig. 32 Local Nusselt number distributions along the flow direction of the test section.

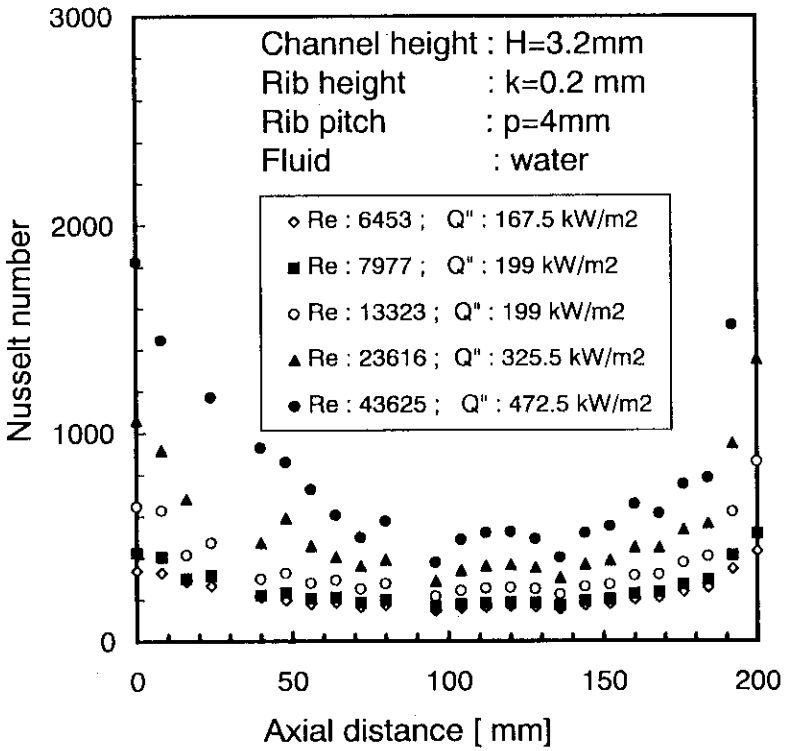

Fig. 33 Local Nusselt number distributions along the flow direction of the test section.

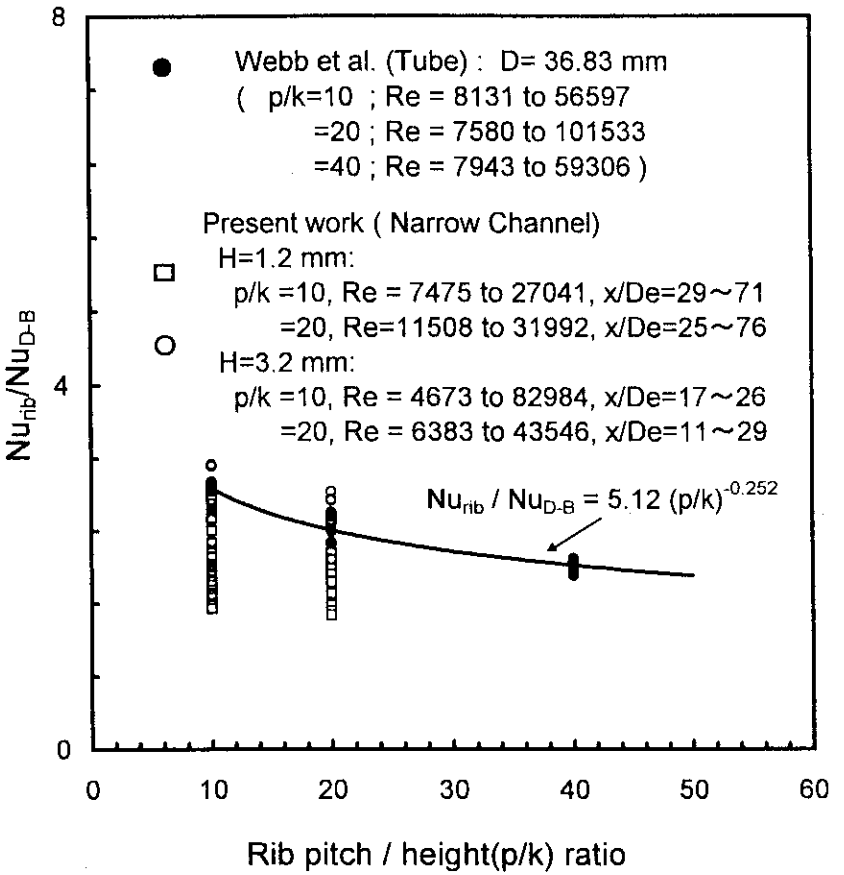

Fig. 34 Nusselt number predictions from the experimental data with the data of Webb et al. for the k/D_e=0.09, k/D_e=0.04, w/k=1.0 channel geometry and for the k/D=0.02, w/k=0.52 tube geomerty with varying p/k ratios.

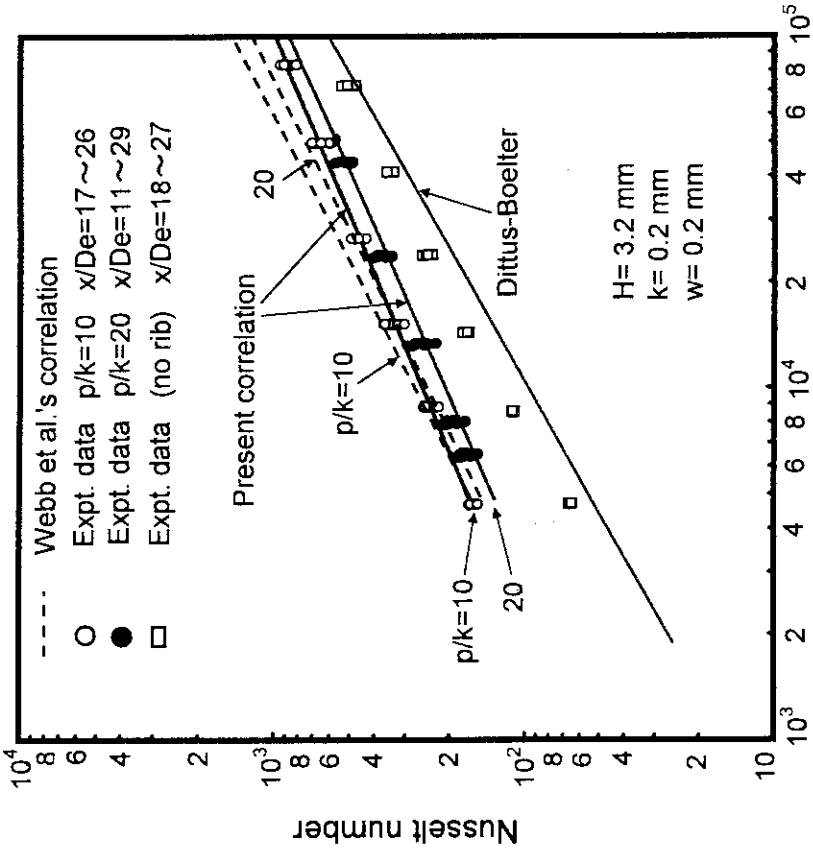

Fig. 36 Comparison of heat transfer correlations with Webb et al.

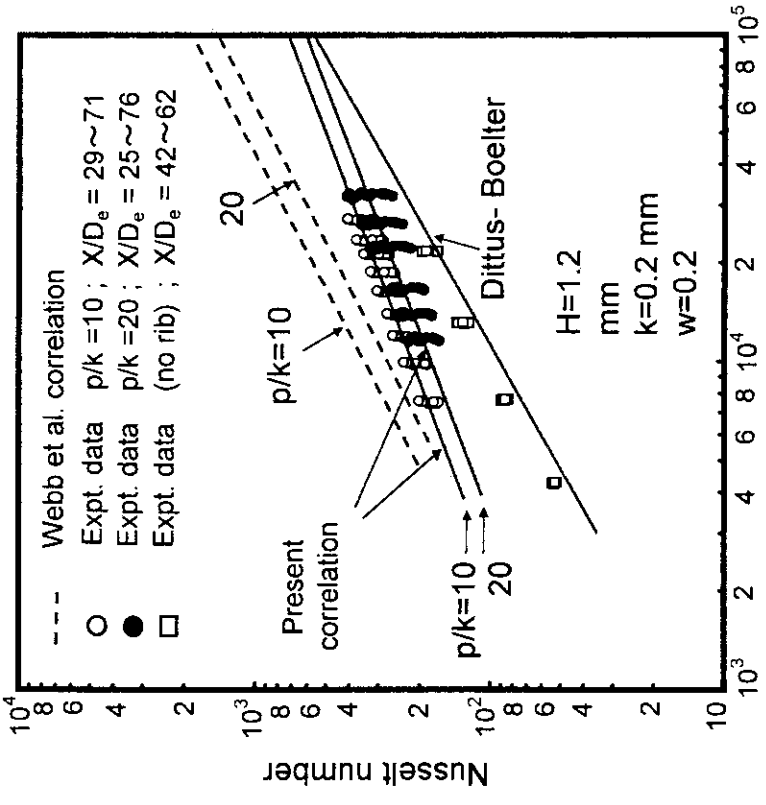

Fig. 35 Comparison of heat transfer correlations with Webb et al.

Table 1 Investigations cited in this study [a]

Study	Tubes tested	Type	Fluid	Expt. condition	f	N-ISO-f	HT
1. Li et al. [6]	20	ind	W	E.H.	20	0	20
2. Webb [7]	5	rib	A,W	E.H.	5	5	5
3. Nakayama et al. [8]	6	ind	W	E.H.	6	0	6
4. Yoshitomi et al. [9]	18	ind	W	E.H.	18	0	18
5. Withers I [10]	13	ind	W	T=Const	13	0	13
6. Withers II [11]	13	ind	W	T=Const	13	0	13
7. Gee and Webb [12]	3	rib	Air	E.H.	3	3	3
8. Berger and Whitehead [13]	3	rib	Air	E.H.	3	0	3
9. Migai and Bystrov [14]	10	ind / fl	Air	T=Const	10	0	10
10. Kalinin et al. [15]	10	ind	Air	W.cooled	10	0	10
11. Bolla et al. [16]	1	rib	He, N_2	W.heated	1	0	1
12. Ganeshan and Rao [17]	7	ind	W	W.heated	7	0	7
13. Gupta and Rao [18]	5	ind	W	W.heated	5	0	5
14. Nunner [19]	4	rib	Air	W.heated	4	0	4
15. Sams [20]	13	coil	Air	E.H.	13	0	13
16. Kumar and Judd [21]	14	coil	W	E.H.	0	14	14
17. Novozhilov and Migai [22]	10	coil	Air	E.H.	10	0	10
18. Snyder [23]	11	coil	W	E.H.	11	0	11
19. Sethumadhavan and Rao [24]	8	coil	W	W.heated	8	8	8
20. Chiou [3]	15	coil	Oil	W.cooled	0	15	15
21. Molloy [25]	1	coil	Air	E.H.	1	0	1
22. Ravigururajan [26]	5	coil	Air	W.cooled	5	0	5
23. Mehta and Rao [27]	8	ind	W	W.heated	8	0	8
24. Ravigururajan and Bergles [5]	4	ind	W	E.H.	4	4	4
25. Zhang et al. [4]	32	coil	Air	W.cooled	32	0	32
26. Cunningham and Milne [28]	3	ind	W	W.heated	3	0	0
27. Mendes and Mauricio [29]	3	rib	W	Sublimation	0	3	3
28. Yampolsky et al. [30]	4	flute	W	W.heated	0	1	1
29. Scaggs et al. [31]	3	3d	W	ISO	3	0	0
30. Scaggs et al. [31]	3	3d	W	ISO	6	0	0
31. Newson and Hodgson [32]	24	flute	W	W.heated	0	24	24
32. Sutherland and Miller [33]	1	rib	Stm	E.H.	0	1	1
33. Smith and Gowen [34]	2	3d	A,W,Gly	E.H.	0	2	2
34. Takahashi et al. [35]	3	3d	W	E.H.	2	0	2
35. Obot and Esen [36]	24	all	Air	E.H.	4	24	24

[a] E.H.= electrical heating, A = air, Gly = glycerin, Stm = steam, W = water

ISO = isothermal, HT = heat transfer

Table 2 Major parameters and conditions of the expt.

Type	H	p / k	k / D_e	Expt. condition
Smooth	1.2	—	0.09	N. H
Smooth	1.2	—	0.09	N. H, E.H.
Smooth	2.97	—	0.04	N. H
Smooth	2.97	—	0.04	N. H, E.H.
Square ribs	3.24	10	0.03	N. H
Square ribs	3.24	10	0.03	N. H, E.H.
Square ribs	1.2	10	0.09	N. H
Square ribs	1.2	10	0.09	N. H, E.H.
Square ribs	3.24	20	0.03	N. H
Square ribs	3.24	20	0.03	N. H, E.H.
Square ribs	1.2	20	0.09	N. H
Square ribs	1.2	20	0.09	N. H, E.H.

*N.H = Non heating , E.H. = electrical heating

Table 3 Range and accuracy of pressure gauges, flow meters, pump, voltmeter and ammeter

Category	Accuracy	Range
Pressure Tap	± 0.3% FS	0 -10Kg_f/cm^2
	± 0.2% FS	0 -0.3Kg_f/cm^2
	± 0.2% FS	0 -5Kg_f/cm^2
	± 0.2% FS	0 -0.2Kg_f/cm^2
	± 0.3% FS	0 -2Kg_f/cm^2
	± 0.2% FS	0 -0.3Kg_f/cm^2
	± 0.2% FS	1.2Kg_f/cm^2
Flow meter	± 0.25% FS	0 -2m^3 / h
	± 0.25% FS	0 -15m^3 / h
Pump	± 0.2% FS	0 -10Kg_f/cm^2
Voltage		0 - 60 V
Current		0 - 300 A

Table 4 Thermocouple range and accuracy

Location		Thermocouple no.	Accuracy	Range
Surface	0mm	TT01	JIS 0.4	0 - 650 ℃
	10mm	TT02	JIS 0.4	0 - 650 ℃
	20mm	TT03	JIS 0.4	0 - 650 ℃
	30mm	TT04	JIS 0.4	0 - 650 ℃
	40mm	TT05	JIS 0.4	0 - 650 ℃
	50mm	TT06	JIS 0.4	0 - 650 ℃
	60mm	TT07	JIS 0.4	0 - 650 ℃
	70mm	TT08	JIS 0.4	0 - 650 ℃
	80mm	TT09	JIS 0.4	0 - 650 ℃
	90mm	TT10	JIS 0.4	0 - 650 ℃
	100mm	TT11	JIS 0.4	0 - 650 ℃
	110mm	TT12	JIS 0.4	0 - 650 ℃
	120mm	TT13	JIS 0.4	0 - 650 ℃
	130mm	TT14	JIS 0.4	0 - 650 ℃
	140mm	TT15	JIS 0.4	0 - 650 ℃
	150mm	TT16	JIS 0.4	0 - 650 ℃
	160mm	TT17	JIS 0.4	0 - 650 ℃
	170mm	TT18	JIS 0.4	0 - 650 ℃
	180mm	TT19	JIS 0.4	0 - 650 ℃
	190mm	TT20	JIS 0.4	0 - 650 ℃
	200mm	TT21	JIS 0.4	0 - 650 ℃
	210mm	TT22	JIS 0.4	0 - 650 ℃
	220mm	TT23	JIS 0.4	0 - 650 ℃
	230mm	TT24	JIS 0.4	0 - 650 ℃
	240mm	TT25	JIS 0.4	0 - 650 ℃
	250mm	TT26	JIS 0.4	0 - 650 ℃
Heater		TT27	JIS 0.4	0 - 650 ℃
		TT28	JIS 0.4	0 - 650 ℃
		TT29	JIS 0.4	0 - 650 ℃
Inlet		TT30	JIS 0.4	0 - 650 ℃
		TT31	JIS 0.4	0 - 650 ℃
		TT32	JIS 0.4	0 - 650 ℃
Outlet		TT33	JIS 0.4	0 - 650 ℃
		TT34	JIS 0.4	0 - 650 ℃
		TT35	JIS 0.4	0 - 650 ℃

Table 5 Experimental conditions

Fluid	Water
Reynolds number	2,414 to 98,485
Flow velocity	up to 25 m/s
Inlet temperature	up to 15℃
Heat flux	up to 0.4725 MW/m^2
System pressure	up to 1.5MPa
Flow direction	Vertical
Flow condition	Fully developed turbulent flow
Heating condition	Uniform heating from one side

Appendix

Experimental data

The data points in the graphical comparisons presented in chapt.5 were carefully taken from the referenced articles/papers [41& 42]. In this appendix, the referenced works are first identified by the tube designations and present works are identified by the channel number. The physical rib and tube/channel dimensions are given in a listed form and the experimental data both the tubes and channels are followed by the tabulated data points for the particular tube/channel as read from the figures of the given works.

Tubes of Webb et al. (1971) :

Tube designation :

Webb et al. 02/10 (k/D=0.02,p/k=10, w/k=0.52)
of Figure 7 and Figure 34

Major Parameters :

Rib width	: w=0.38 mm
Rib height	: k=0.7366 mm
Rib pitch	: p= 7.366 mm
Tube diameter	: D=36.83 mm

Experimental data :

Tables 1- W and 2-W

Narrow channel (1997)

Shafiqul et al. : Channel -1 (k/D_e=0.09, p/k=10, w/k=1.0)
of Figure 7 , Figure 8, Figure 34 and Figure 35

Major parameters :

Rib width	: w=0.2 mm
Rib height	: k=0.2 mm
Rib pitch	: p= 2 mm
Channel height	: H=1.2 mm

Experimental data :

Tables 1- E and 2- E

Table 1- W Friction data for Tube 02/10

Point	Re	f_T
1	6903	0.02648
2	7234	0.02935
3	8620	0.02935
4	10035	0.03144
5	10153	0.0318
6	13920	0.0333
7	14084	0.03446
8	25563	0.03486
9	35460	0.03566
10	48054	0.03649
11	51545	0.03566
12	65119	0.03415
13	67443	0.03608
14	94656	0.03446

Table 2 - W Heat transfer data for tube 02/10

Point	Re	Nu
1	8131	172
2	12385	244
3	22217	390
4	40800	611
5	56597	738

Table 1 - E Friction data for channel - 1
(X/D_e=41-to-66)

Point	Re	f_T
1	6887	0.02
2	8551	0.0187
3	10288	0.0176
4	12306	0.0165
5	14620	0.0155
6	16440	0.0152
7	18320	0.015
8	20328	0.0145
9	23494	0.0139

Table 2 - E Heat transfer data for channel -1
(X/D_e=29-to-71)

Point	Re	Nu	Point	Re	Nu	Point	Re	Nu
1	7475	169	26	13847	260	51	21222	289
2	7493	184	27	13864	255	52	21251	277
3	7507	179	28	13882	234	53	21297	300
4	7522	170	29	13906	229	54	21326	342
5	7540	167	30	13948	245	55	21383	349
6	7573	175	31	13973	276	56	23379	286
7	7591	193	32	16261	238	57	23408	361
8	7629	202	33	16286	291	58	23427	345
9	9782	187	34	16304	281	59	23445	302
10	9804	215	35	16321	259	60	23475	296
11	9821	209	36	16347	248	61	23524	319
12	9839	192	37	16390	264	62	23554	374
13	9861	190	38	16416	300	63	27041	311
14	9900	209	39	16467	306	64	27073	394
15	9923	227	40	18649	256	65	27092	376
16	9968	235	41	18675	315	66	27112	326
17	11805	206	42	18693	308	67	27144	324
18	11827	238	43	18711	279	68	27196	355
19	11845	234	44	18738	263	69	27229	409
20	11862	214	45	18783	284	70	27294	407
21	11885	210	46	18810	324			
22	11925	227	47	18865	328			
23	11948	253	48	21158	270			
24	11995	261	49	21186	335			
25	13823	220	50	21204	324			

Tubes of Webb et al. (1971) :

Tube designation :

Webb et al. 02/20 (k/D=0.02, p/k=20, w/k=0.52)
of Figure 7 and Figure 34

Major Parameters :

Rib width : w=0.38 mm
Rib height : k=0.7366 mm
Rib pitch : p= 14.732 mm
Tube diameter : D=36.83 mm

Experimental data :

Tables 3 -W and 4-W

Narrow channel (1997)

Shafiqul et al. : Channel -2 (k/D_e=0.09, p/k=20, w/k=1.0)
of Figure 7 , Figure 8, Figure 34 and Figure 35

Major parameters :

Rib width : w=0.2 mm
Rib height : k=0.2 mm
Rib pitch : p= 4 mm
Channel height : H=1.2 mm

Experimental data :

Tables 3-E and 4- E

Table 3 - W Friction data for tube 02/20

Point	Re	f_T
1	6512	0.02011
2	8036	0.02255
3	10890	0.02361
4	13598	0.02416
5	18428	0.02472
6	23831	0.02529
7	30108	0.02588
8	44799	0.02648
9	54012	0.02709
10	82269	0.02772
11	101533	0.02804
12	125308	0.02902
13	142501	0.02902

Table 4 - W Heat transfer data for tube 02/20

Point	Re	Nu
1	7580	134
2	13920	235
3	34641	482
4	59306	697
5	101533	1008

Table 3 - E Friction data for channel - 2
(X/D_e=45-to-74)

Point	Re	f_T
1	10791	0.01309
2	12845	0.01237
3	14679	0.01225
4	17141	0.01167
5	19792	0.01108
6	23013	0.01083
7	27679	0.01027

Table 4 - E Heat transfer data for channel - 2
(X/D_e= 25-to-76)

Point	Re	Nu	Point	Re	Nu	Point	Re	Nu
1	11508	224	31	16799	204	60	32090	263
2	11531	202	32	16809	218	61	32133	342
3	11553	165	33	16815	261	62	31321	390
4	11573	198	34	16853	251	63	32392	282
5	11687	170	35	22060	326	64	31855	375
6	11499	224	36	22097	269	65	32507	279
7	11740	173	37	22132	219	66	32623	293
8	11792	176	38	22163	279	67	32643	319
9	11805	188	39	21609	323	68	32655	403
10	11814	219	40	22350	230	69	32729	359
11	11847	215	41	21981	304			
12	13731	248	42	22433	232			
13	13755	215	43	22518	241			
14	13779	178	44	22533	259			
15	13800	216	45	22544	313			
16	13923	181	46	22597	293			
17	13696	237	47	26247	357			
18	13979	185	48	26286	294			
19	14035	191	49	26323	237			
20	14047	203	50	26355	309			
22	14055	239	51	26558	250			
23	14090	233	52	26115	332			
24	16476	270	53	26648	253			
25	16501	233	54	26738	263			
26	16526	192	55	26751	283			
27	16548	238	56	26759	351			
28	16680	196	57	26817	322			
29	16403	257	58	31992	410			
30	16739	198	59	32043	329			

Tubes of Webb et al. (1971) :

Tube designation :

Webb et al. 02/40 (k/D=0.02, p/k=40, w/k=0.52)
of Figure 7 and Figure 34

Major Parameters :

Rib width : w=0.38 mm
Rib height : k=0.7366 mm
Rib pitch : p= 29.464 mm
Tube diameter : D=36.83 mm

Experimental data :

Tables 5-W and 6- W

Narrow channel (1997)

Shafiqul et al. : Channel - 3 (k/D_e=0.04, p/k=10, w/k=1.0)
of Figure 7 , Figure 9, Figure 34 and Figure 36

Major parameters :

Rib width : w=0.2 mm
Rib height : k=0.2 mm
Rib pitch : p= 2 mm
Channel height : H=3.24mm

Experimental data :

Tables 5- E and 6-E

Table 5 - W Friction data for tube 02/40

Point	Re	f_T
1	6512	0.01493
2	6903	0.01528
3	8323	0.01563
4	8323	0.01637
5	8520	0.01563
6	11018	0.01655
7	13758	0.01674
8	18002	0.01637
9	23554	0.01674
10	24395	0.01694
11	30820	0.01713
12	44278	0.01713
13	44799	0.01694
14	51545	0.01733
15	79434	0.01773
16	99187	0.01794
17	125308	0.01835
18	140845	0.01878

Table 6 - W Heat transfer data for tube 02/40

Point	Re	Nu
1	7943	111
2	14084	185
3	21452	270
4	33841	385
5	59306	569

Table 5 - E Friction data channel - 3
(X/D_e=17-to-28)

Point	Re	f_T	Point	Re	f_T
1	4546	0.0234	10	22263	0.0159
2	5501	0.0217	11	25524	0.0158
3	6300	0.0207	12	32793	0.0159
4	7377	0.0194	13	39207	0.0154
5	8470	0.019	14	47113	0.015
6	9750	0.0185	15	54963	0.0151
7	12039	0.0175	16	63358	0.015
8	14584	0.0172	17	77508	0.0143
9	17339	0.0167			

Table 6 - E Heat transfer data for channel -3
(X/D_e=17-to-26)

Point	Re	Nu	Point	Re	Nu
1	4673	165	29	49750	675
2	4678	164	30	49772	608
3	4683	157	31	49781	650
4	4689	154	32	49809	707
5	4693	164	33	82984	864
6	4699	153	34	83141	940
7	8828	249	35	83188	940
8	8835	253	36	83234	824
9	8843	236	37	83260	814
10	8851	229	38	83325	909
11	8857	242			
12	8865	221			
13	8870	249			
14	15180	341			
15	15189	365			
16	15200	337			
17	15212	321			
18	15219	349			
19	15230	302			
20	15237	363			
21	26544	479			
22	26586	445			
23	26612	470			
24	26628	432			
25	26636	464			
26	26658	496			
27	49713	596			
28	49727	698			

Narrow channel (1997)

Shafiqul et al. : Channel - 4 (k/D_e=0.04, p/k=20, w/k=1.0) of Figure 7 , Figure 9, Figure 34 and Figure 36

Major parameters :

Rib width : w=0.2 mm
Rib height : k=0.2 mm
Rib pitch : p= 4 mm
Channel height : H=3.24mm

Experimental data :

Tables 7- E and 8- E

Table 7 - E Friction data for channel - 4 (X/De=18-to-29)

Point	Re	f_T
1	3790	0.02322
2	4770	0.01946
3	5774	0.01878
4	6932	0.01739
5	8184	0.01700
6	9951	0.01618
7	12093	0.01559
8	14994	0.01512
9	18532	0.01464
10	22056	0.01437
11	26109	0.01410
12	32684	0.01393
13	39085	0.01367
14	46221	0.01347
15	57738	0.01321
16	69762	0.01305
17	83886	0.01285

Table 8 - E Heat transfer data for channel - 4 (X/D_e=11-to-29)

Point	Re	Nu	Point	Re	Nu	Point	Re	Nu
1	6383	180	19	8057	185	37	23729	339
2	6394	185	20	8068	172	38	23757	361
3	6422	165	21	8076	194	39	23785	367
4	6439	174	22	8083	202	40	23802	353
5	6485	158	23	13219	280	41	23827	370
6	6497	163	24	13235	294	42	23834	388
7	6508	166	25	13286	251	43	43546	497
8	6517	165	26	13314	277	44	43627	576
9	6526	154	27	13387	243	45	43832	487
10	6532	172	28	13404	255	46	43875	519
11	6538	178	29	13421	257	47	43918	524
12	7891	205	30	13432	252	48	43942	491
13	7905	212	31	13443	226	49	43972	517
14	7939	186	32	13448	263	50	43977	551
15	7960	198	33	13453	273			
16	8017	179	34	23469	404			
17	8032	184	35	23558	362			
18	8046	186	36	23606	391			

Narrow channel (Smooth, 1997)

Channel designation :

Shafiqul et al. : Channel - 5 Figure 8 and Figure 35

Major parameter :

Channel height : H= 1.2 mm

Experimental data :

Tables 9-E and 10-E

Table 9 - E Friction data for channel - 5
(X/D_e=41-to-67)

Point	Re	f_T	$f_{blasius}$	$f_{laminar}$=1.4*16 / Re
1	2415	0.0134	0.0113	0.02240
2	2791	0.0124	0.0109	0.01867
3	3254	0.0117	0.0105	0.01600
4	3982	0.0108	0.0099	0.01400
5	4741	0.0103	0.0095	0.01244
6	5528	0.0097	0.0092	0.01120
7	7086	0.0088	0.0086	0.00896
8	7967	0.0084	0.0084	0.00747
9	9529	0.008	0.008	
10	12049	0.0073	0.0075	
11	16043	0.0067	0.007	
12	19901	0.0061	0.0066	
13	24695	0.0057	0.0063	
14	28847	0.0054	0.0061	
15	33480	0.0052	0.0058	

Table 10 - E Heat transfer data for channel -5
(X/D_e=42-to-62)

Point	Re	Nu
1	4263	53
2	4278	54
3	4286	53
4	4301	52
5	4309	53
6	7647	86
7	7666	90
8	7675	88
9	7694	84
10	7704	86
11	13066	129
12	13091	139
13	13103	137
14	13127	124
15	13140	131
16	21719	196
17	21730	169
18	21744	168
19	21759	188

Narrow channel (Smooth , 1997)

Channel designation :
Shafiqul et al. : Channel -6 Figure 9 and 36

Major parameter :

Channel height : H=2.97 mm

Experimental data :

Tables 11- E and 12- E

Table 11 -E Friction data for channel - 6
(X/D_e=18-to-30)

Point	Re	f_T	$f_{blasius}$	$f_{laminar}$=1.4*16/Re
1	4826	0.008693	0.009478	0.02240
2	5824	0.008579	0.009043	0.01867
3	6808	0.008407	0.008697	0.01400
4	8242	0.008141	0.008291	0.01120
5	10181	0.007842	0.007865	0.00747
6	12297	0.007626	0.007502	
7	14351	0.007450	0.007218	
8	20151	0.006867	0.006631	
9	24381	0.006730	0.006322	
10	30171	0.006230	0.005994	
11	28067	0.003591	0.006104	
12	36292	0.006092	0.005724	
13	41338	0.006106	0.005540	
14	54138	0.005773	0.005179	
15	98458	0.005202	0.004460	

Table 12 - E Heat transfer data for channel - 6
(X/D_e=18-to-27)

Point	Re	Nu	Point	Re	Nu
1	4701	66	19	41082	353
2	4712	66	20	41156	357
3	4717	65	21	41201	335
4	4727	64	22	41217	356
5	4731	64	23	72450	489
6	8566	111	24	72550	538
7	8588	112	25	72588	511
8	8602	109	26	72669	472
9	8608	112	27	72700	512
10	14419	176			
11	14428	169			
12	14446	166			
13	14454	169			
14	23826	247			
15	23859	257			
16	23871	248			
17	23898	233			
18	23908	243			